



Two-Metal Ion Catalysis by Ribonuclease H

Edina Rosta

KING'S
College
LONDON

Department of Chemistry
King's College London

Phosphate Groups as Building Blocks

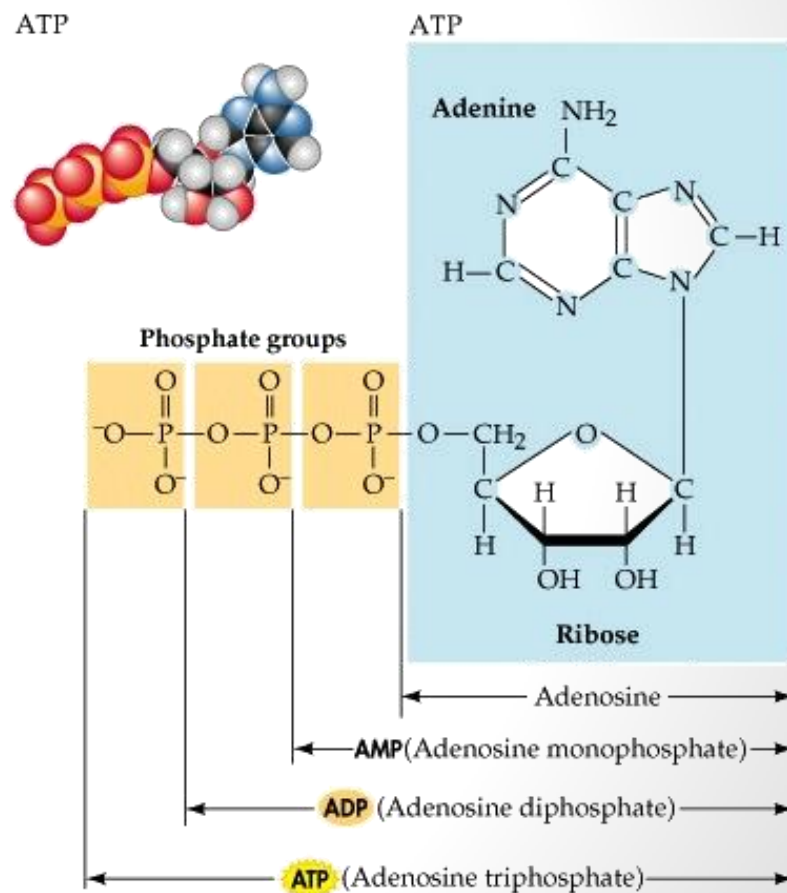


- **Biological importance:**

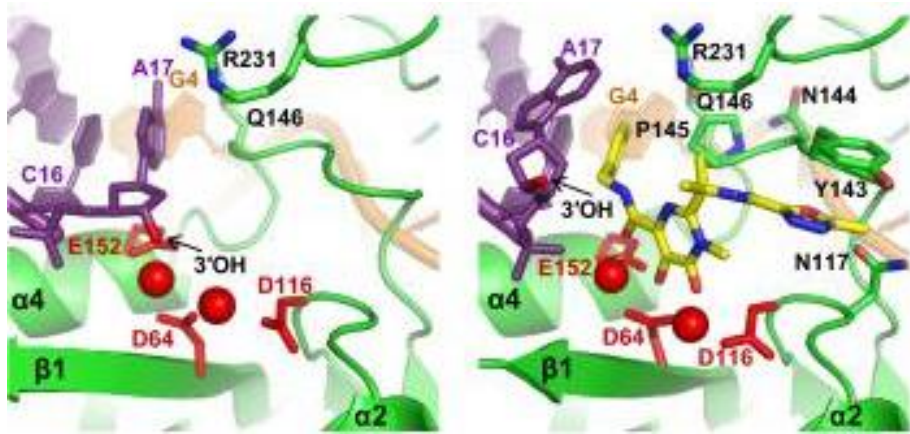
- **Reproduction:**
DNA and RNA hydrolysis, synthesis
Regulation of gene expression
- **Energy storage and transfer:**
ADP/ATP equilibrium provides energy for reactions in the cells
- **Signaling:**
Phosphorylation activates or deactivates proteins in regulatory processes

- **Theoretical importance:**

- **Reaction mechanism**
- Highly charged species
- Solvation effects
- Charge transfer, polarization effects
- Large entropy effects
- **Metal ions in enzymes**

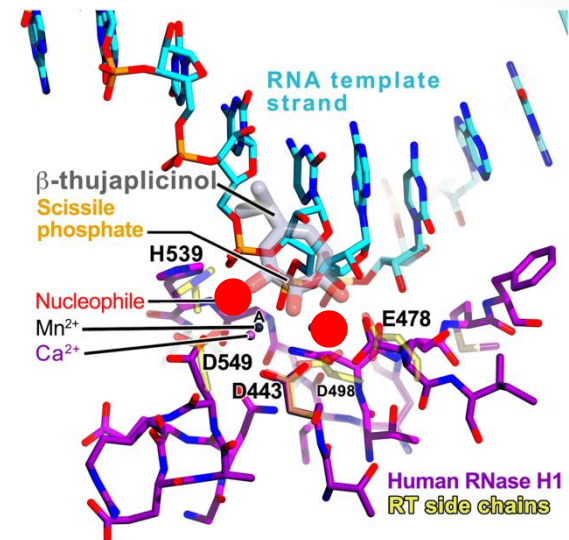


Two-Metal Ion Catalysis



IN active site + Raltegravir
(drug molecule for HIV-IN)

Krishnan, et. al., *PNAS*, 2010
Hare, et. al, *Nature*, 2010



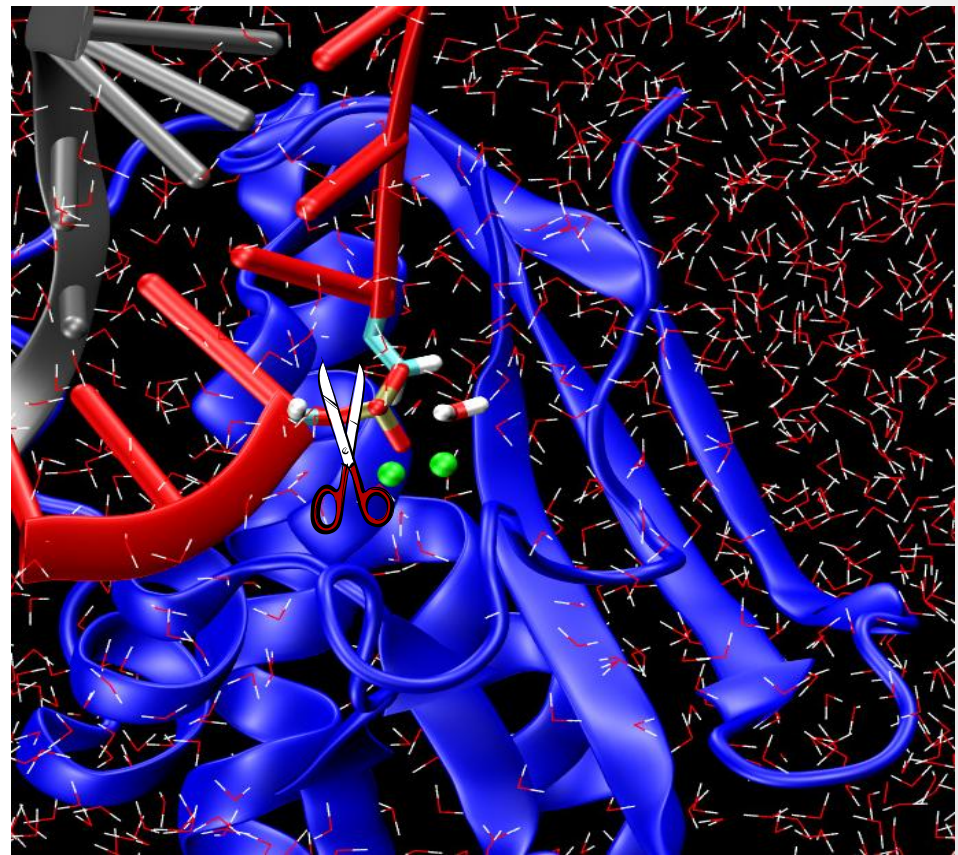
HIV-RT RNase H active site +
inhibitor beta-thujaplicinol
superimposed with human RNase
H active site

Nowotny, et al., *Cell*, 2007
Himmel, et al., *Cell*, 2009

- *Why are metal ions indispensable?*
- *Can we understand their catalytic roles based on quantum chemistry?*

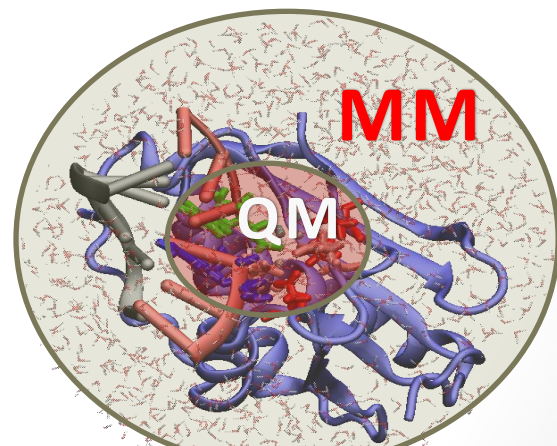
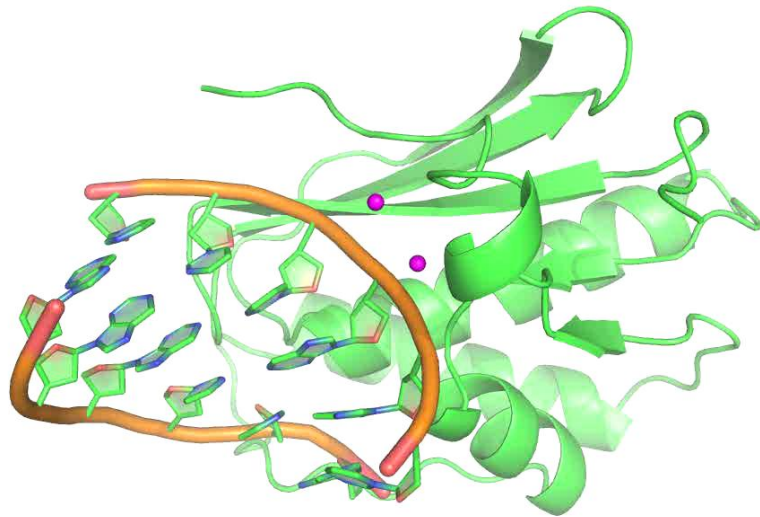
RNase H Catalytic Reaction

- *B. halodurans* RNase H complexed with RNA/DNA duplex substrate
Nowotny, et. al, Cell, 2005
- Crystal structure includes bound Mg²⁺-ions in active site
- Enzyme catalyzes the non-specific cleavage of the RNA backbone phosphate ester bond in the RNA/DNA duplex via hydrolytic mechanism
- Same type of active site is major drug target in HIV-RT

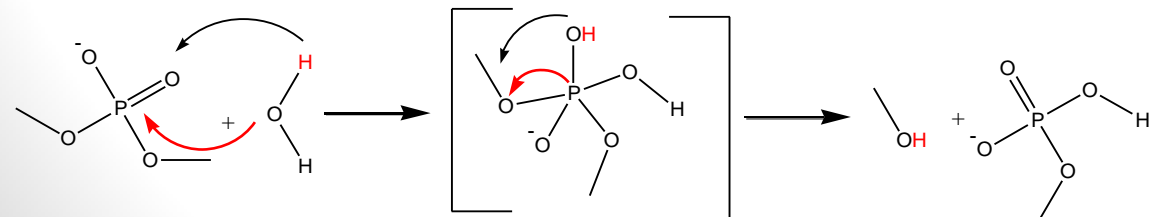


Computational Methods

- NEW QM/MM implementation with **Q-Chem** +CHARMM using full electrostatic embedding
Woodcock et al., J. Comp. Chem., 2007
- Phosphate-diester hydrolysis by attacking water
- DFT B3LYP method
- **Free energy** calculations using Umbrella Sampling



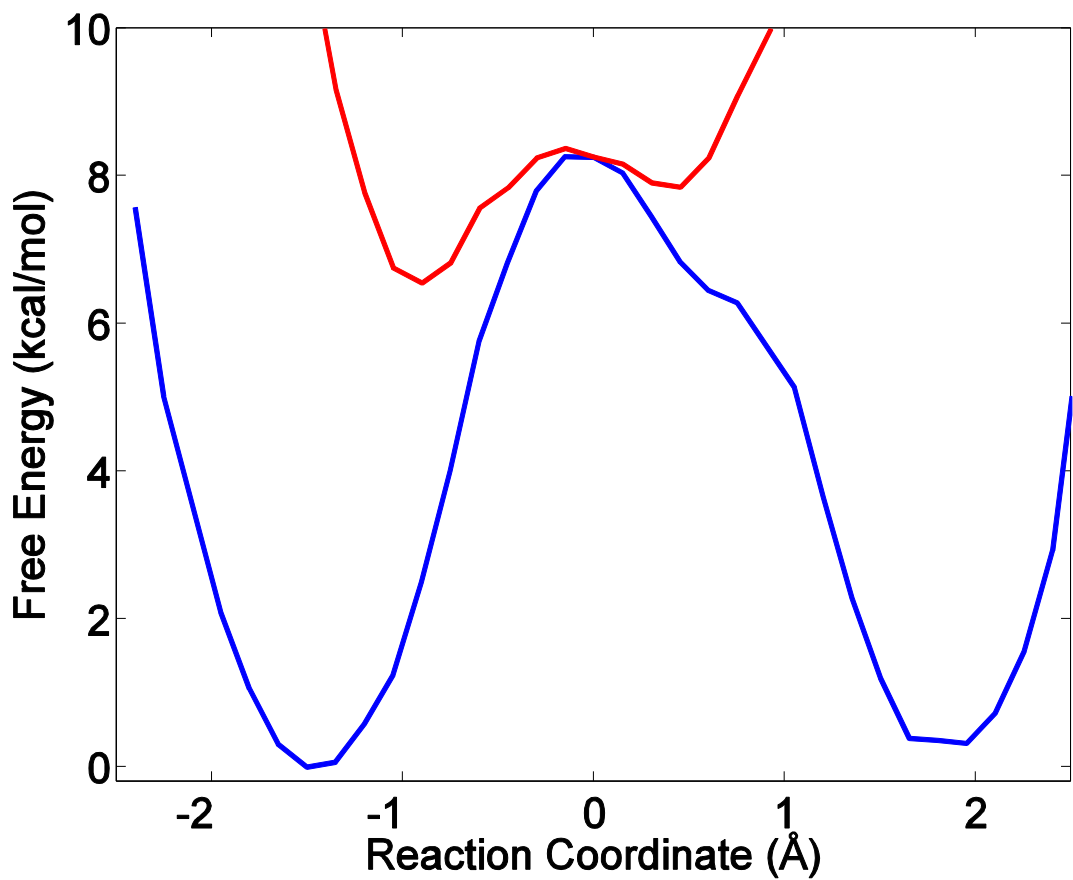
Q-CHEM



Umbrella Sampling

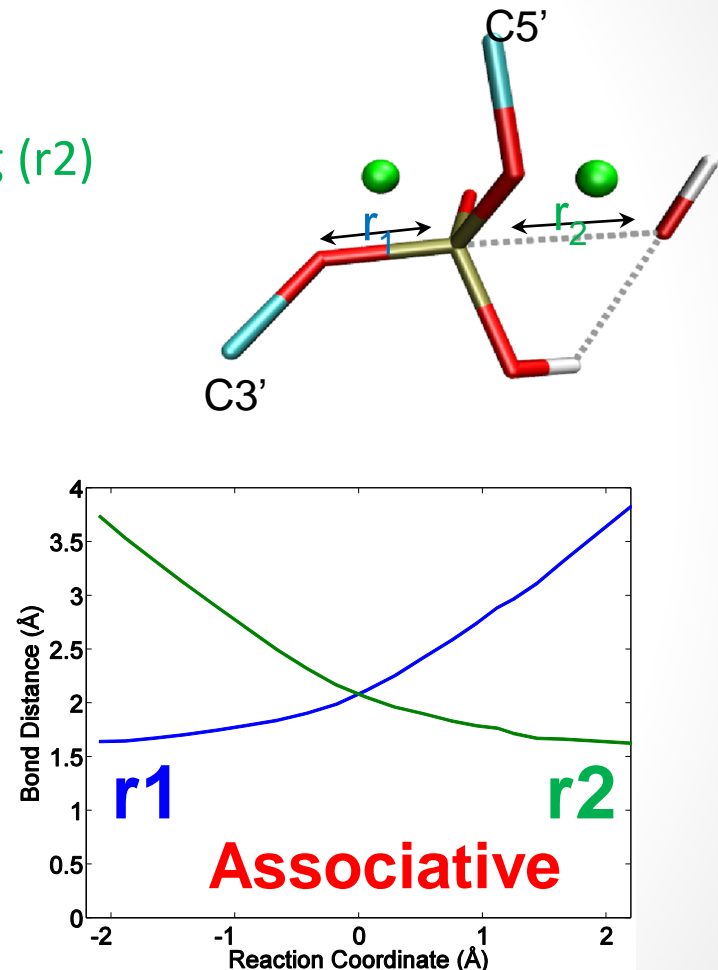
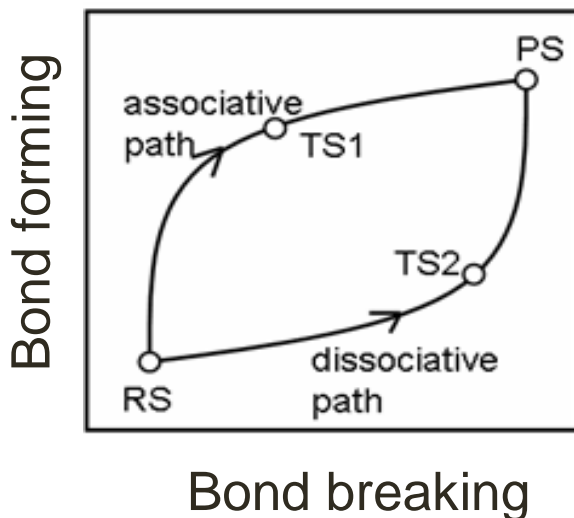
- Run parallel simulations with harmonic constraints moving along the reaction coordinate
- Recover the unbiased free energy surface from combined data using e.g., WHAM

$$E_i(q_A) = U_{pot}(q_A) + \frac{1}{2} k_i (\xi_A - \xi_i)^2$$



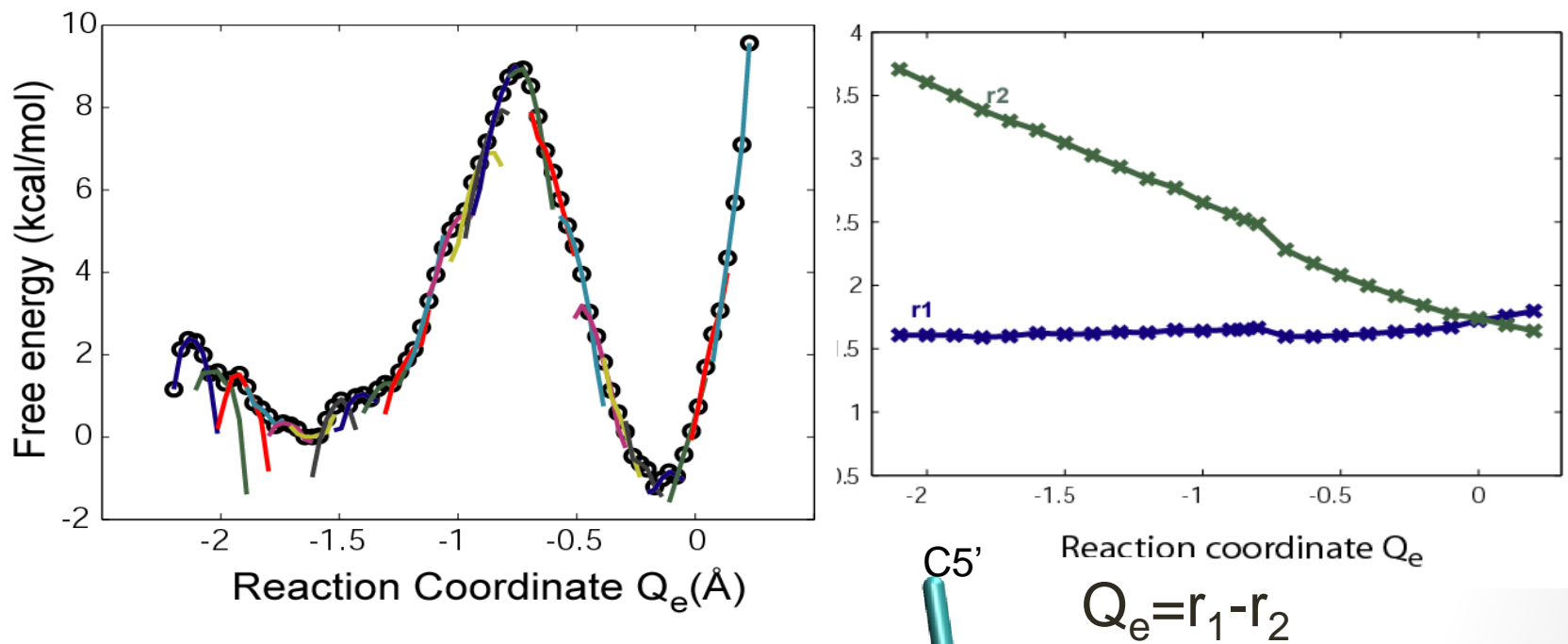
Reaction Coordinate

- 1D coordinate:
$$Q_e = \text{Bond breaking (r1)} - \text{Bond forming (r2)}$$
- Allows to distinguish between associative/dissociative mechanisms

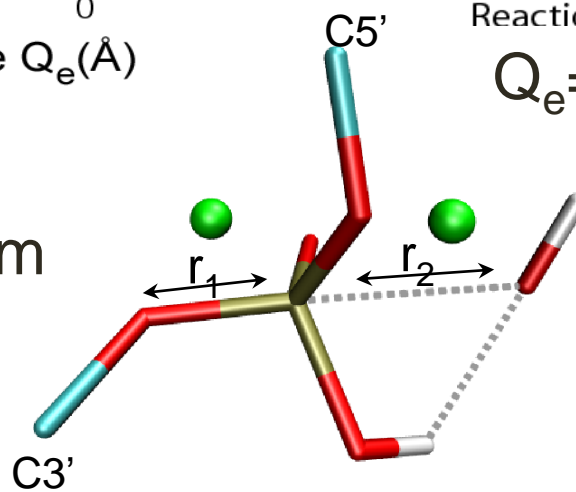


More O'Ferrall-Jencks diagram

Umbrella Sampling along Q_e

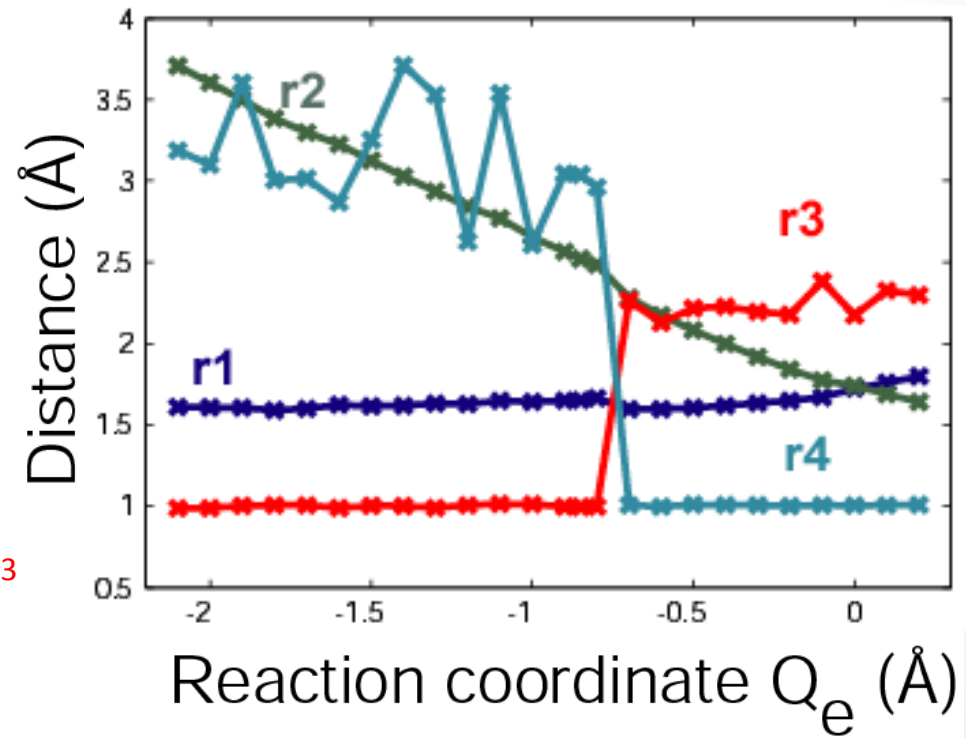
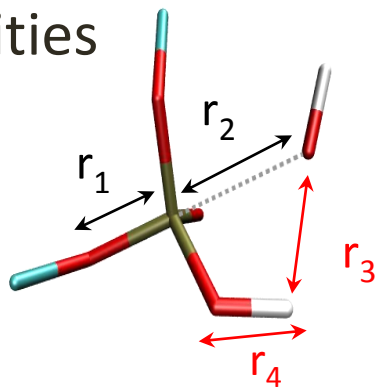


- Associative mechanism



Automated search for discontinuities in atomic distances

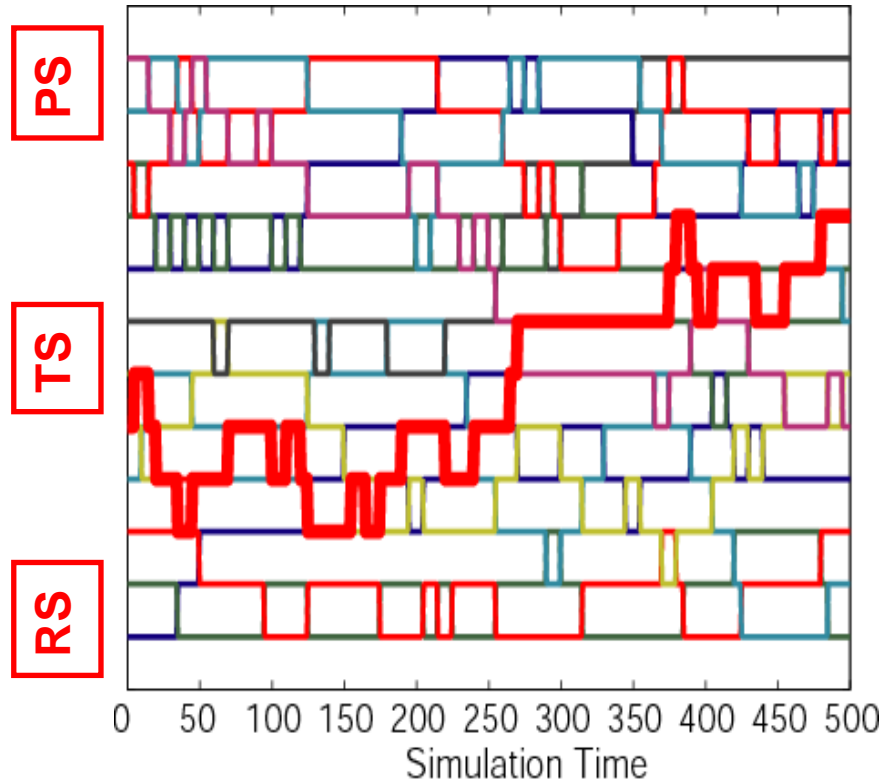
Analyze atomic distances
along umbrella
sampling windows for
discontinuities



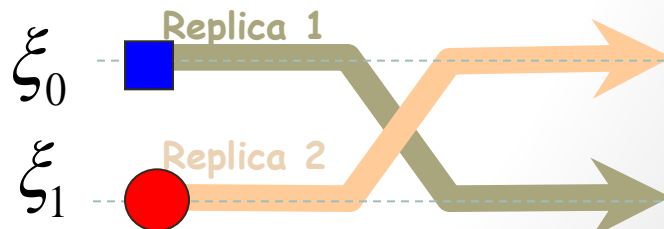
Electron transfer: $Q_e = r_1 - r_2$
Proton transfer: $Q_p = r_3 - r_4$

Hamiltonian Replica Exchange

Why replica exchange? Can we optimize our protocol?



- Running MD at different temperatures in parallel
- Couple the runs in order to speed up lowest temperature's dynamics
- Preserve P_{eq} at each temperature
- Detailed balance condition has to be satisfied

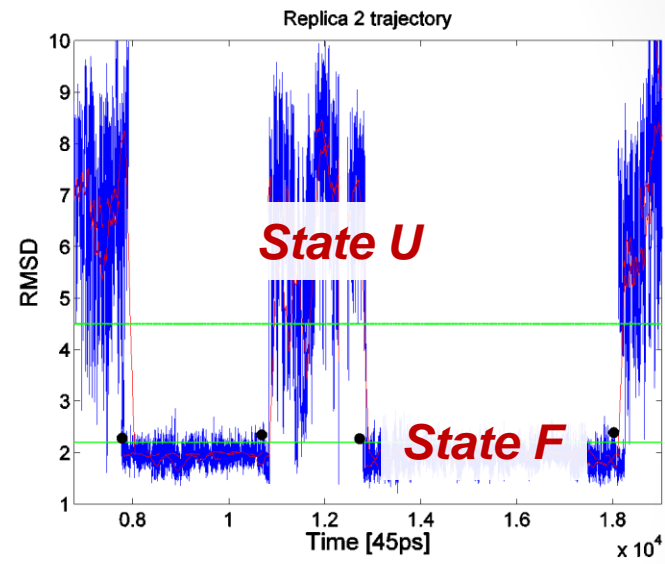
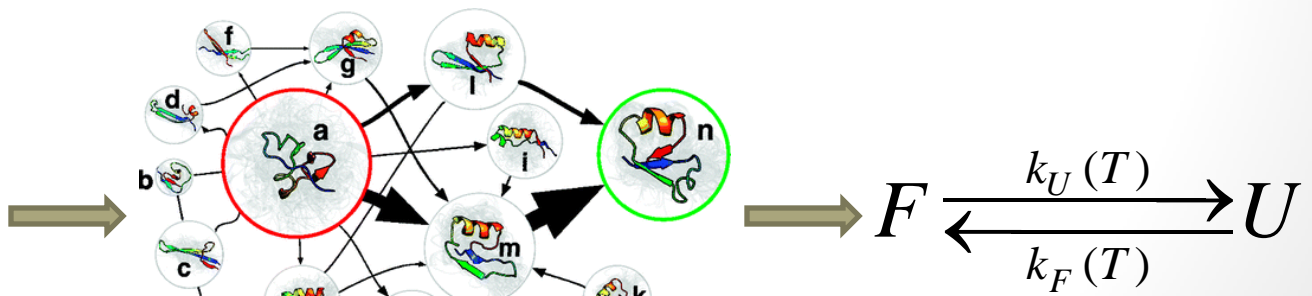
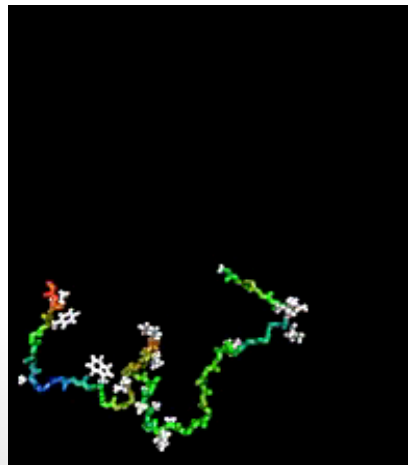


K. Hukushima and K. Nemoto, *J. Phys. Soc. Japan*, 1996
Fukunishi, Watanabe & Takada, *J. Chem. Phys.*, 2002

State Assignment in Protein Folding Simulations

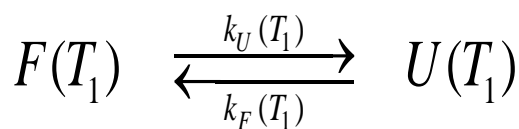
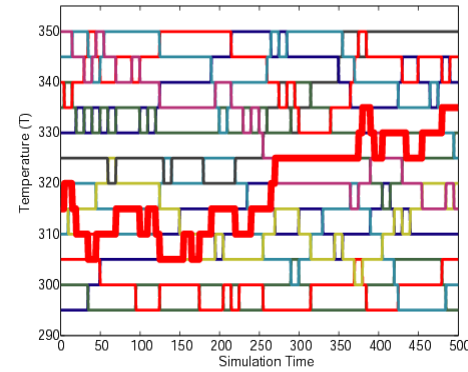
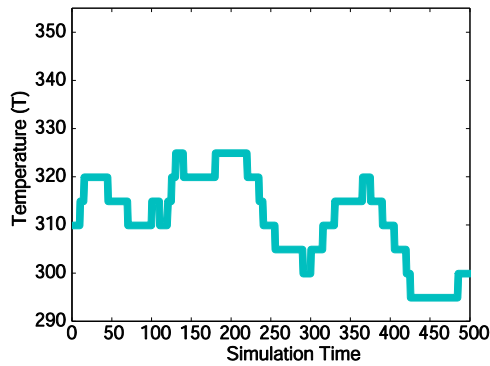
$$\frac{dP_i}{dt}(t) = \sum_{\substack{j=1 \\ (j \neq i)}}^N k_{i \leftarrow j} P_j(t) - \sum_{\substack{j=1 \\ (j \neq i)}}^N k_{j \leftarrow i} P_i(t)$$

Folding@home, V. Pande, Stanford



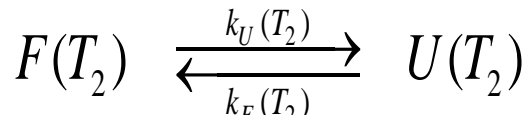
Two-State Kinetic Model of Replica Exchange and Simulated Tempering

W. Zheng, M. Andrec, E. Gallicchio and R. Levy, PNAS, 2007

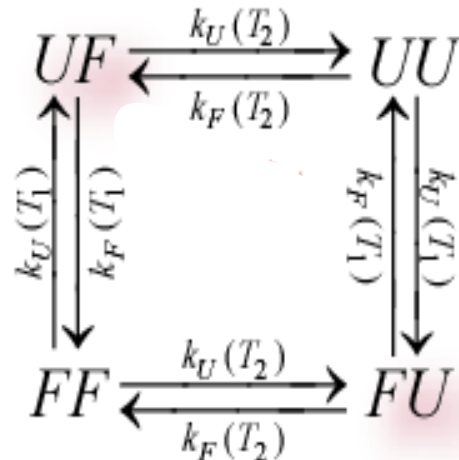


SLOW

preserves p_{eq}

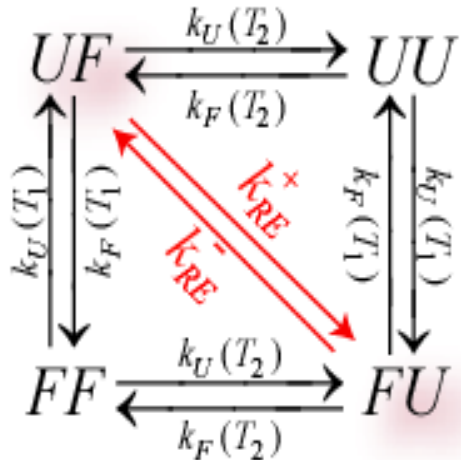


FAST

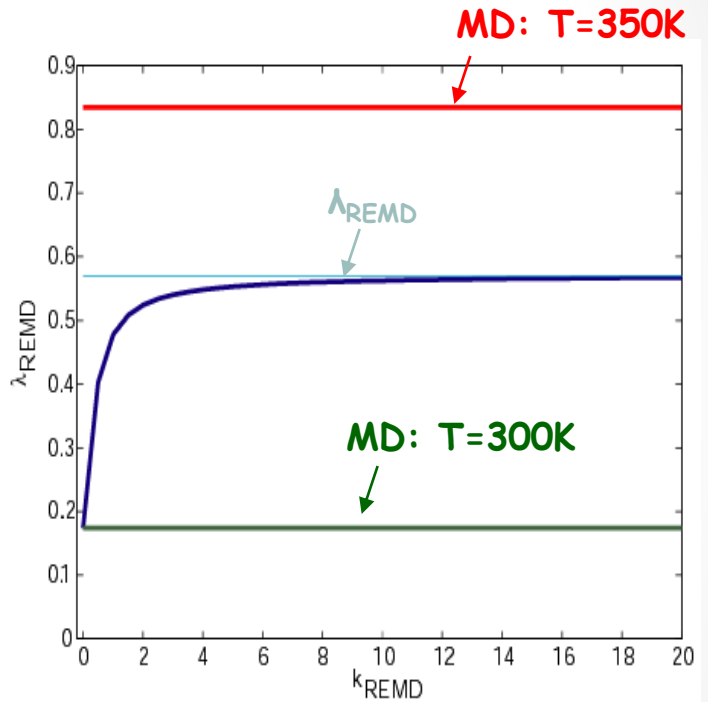


$(L)_{\text{dil}}$

Replica Exchange Rate

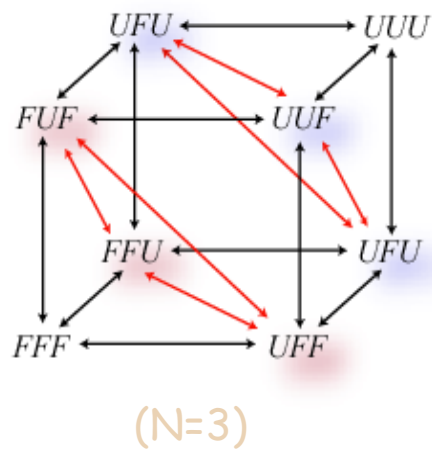
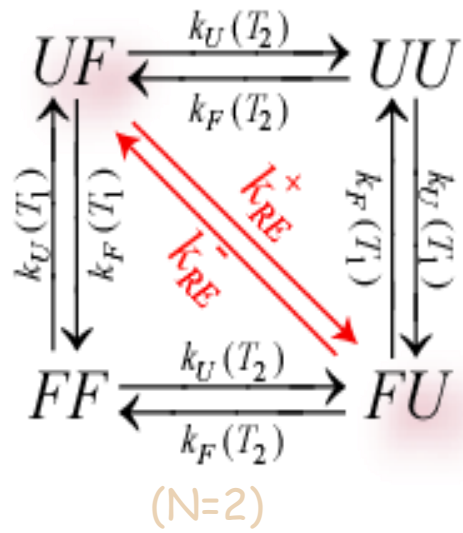


$$k_{RE} \frac{U_i F_j \rightarrow U_j F_i}{\delta t_{xc}} = \frac{p_{acc} U_i F_j \rightarrow U_j F_i}{\delta t_{xc}}$$



$$K = \begin{bmatrix} -k_U(T_1) + k_U(T_2) & k_F(T_1) & k_F(T_2) & 0 \\ k_U(T_1) & -k_F(T_1) + k_U(T_2) + k_{RE}^+ & k_{RE}^- & k_F(T_2) \\ k_U(T_2) & k_{RE}^+ & -k_U(T_1) + k_F(T_2) + k_{RE}^- & k_F(T_1) \\ 0 & k_U(T_2) & k_U(T_1) & -k_F(T_2) + k_F(T_1) \end{bmatrix}$$

Coarse Graining Replica Exchange Coupled States: Fast Exchange Limit



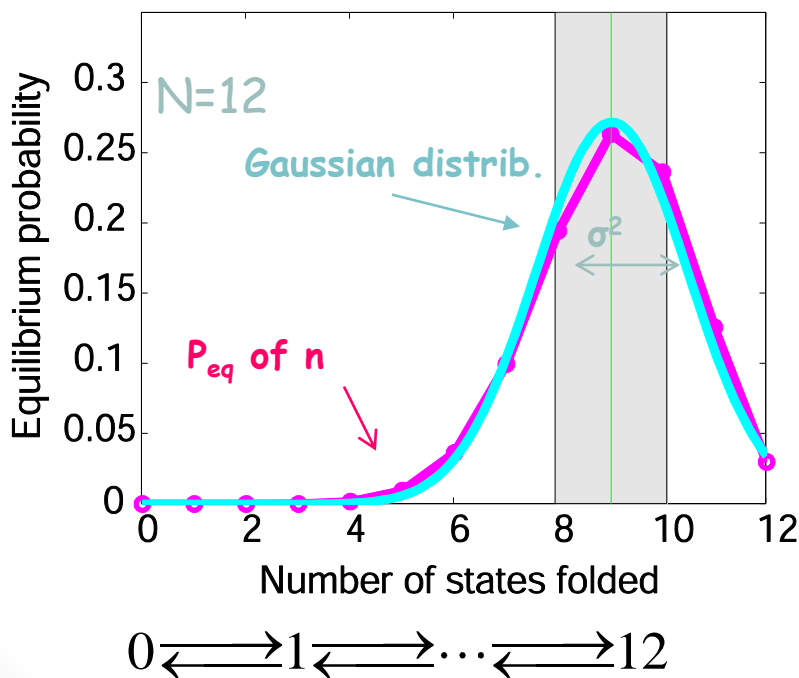
...

N temperatures
(2^N microstates)

$$FF \longleftrightarrow \binom{UF}{FU} \longleftrightarrow UU \quad FFF \longleftrightarrow \binom{FFU}{FUF}{UFF} \longleftrightarrow \binom{FUU}{UFU}{UUU} \longleftrightarrow UUU \quad 0 \longleftrightarrow 1 \longleftrightarrow \dots \longleftrightarrow N$$

Kinetic Theory: Continuum Limit

- Smoluchowski equation for diffusion in a one-dimensional harmonic potential



- Analytic solution for the slowest relaxation rate of the system:

$$\lambda = \frac{D}{\sigma^2} = \frac{K_{n_{\max}-1, n_{\max}}}{\sigma^2}$$

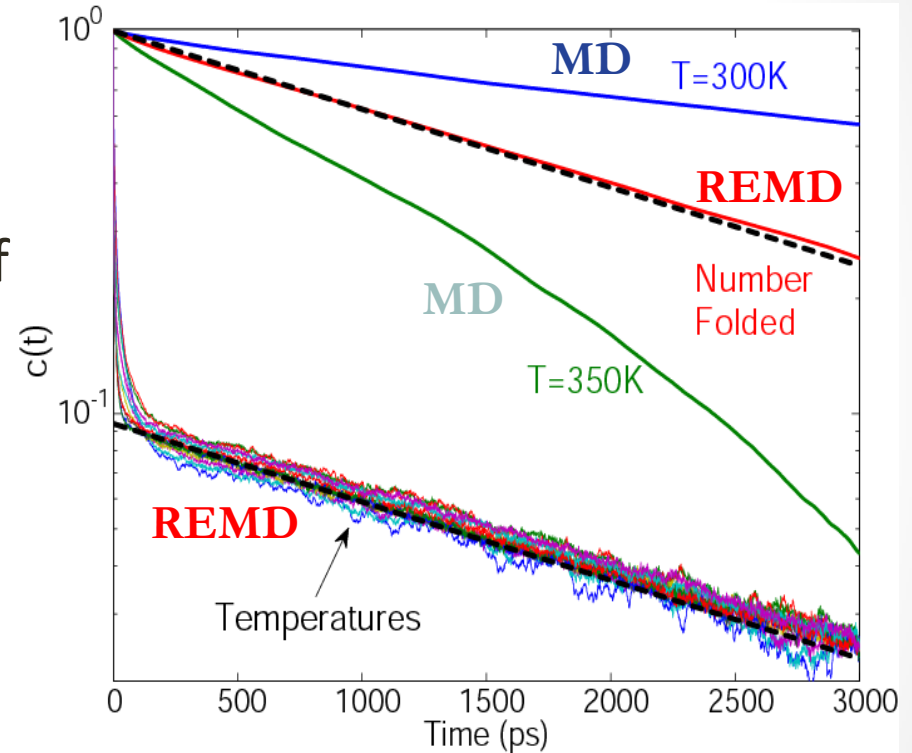
$$\lambda_{REMD} = \frac{\sum_{i=1}^N \lambda(T_i) p_F(T_i) p_U(T_i)}{\sum_{i=1}^N p_F(T_i) p_U(T_i)}$$

Exact for $N \rightarrow \infty$ and $k_{RE} \rightarrow \infty$.

Folding/Unfolding of Ala₅

- All-atom simulations of Ala₅ in explicit water
- State correlation function of all temperatures:

$$c(t) = \frac{\langle s(t)s(0) \rangle_T - \langle s(t) \rangle_T^2}{\langle s(t)^2 \rangle_T - \langle s(t) \rangle_T^2}$$

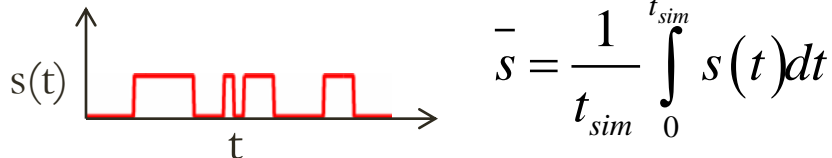


- Fit for λ matches the prediction perfectly using the corresponding folding/unfolding rates!

$$\lambda_{REMD} = \frac{\sum_{i=1}^N \lambda(T_i) p_F(T_i) p_U(T_i)}{\sum_{i=1}^N p_F(T_i) p_U(T_i)}$$

Efficiency of Replica Exchange

- Estimating the mean of the folding state function $s(t)$:



- Efficiency = relative error compared to standard MD simulations using the same computational resources:

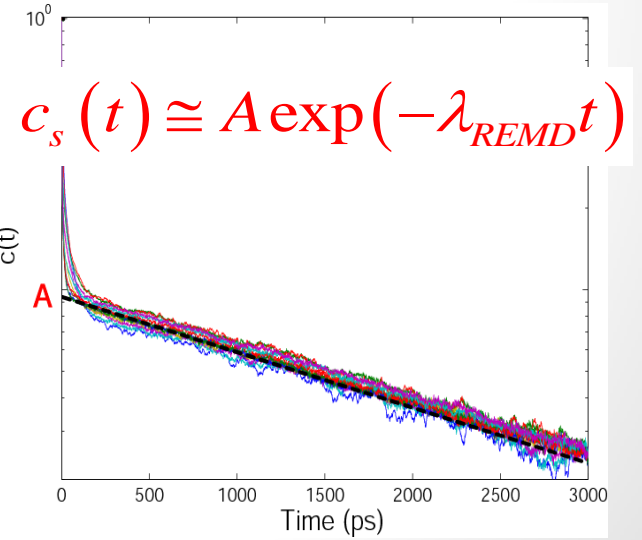
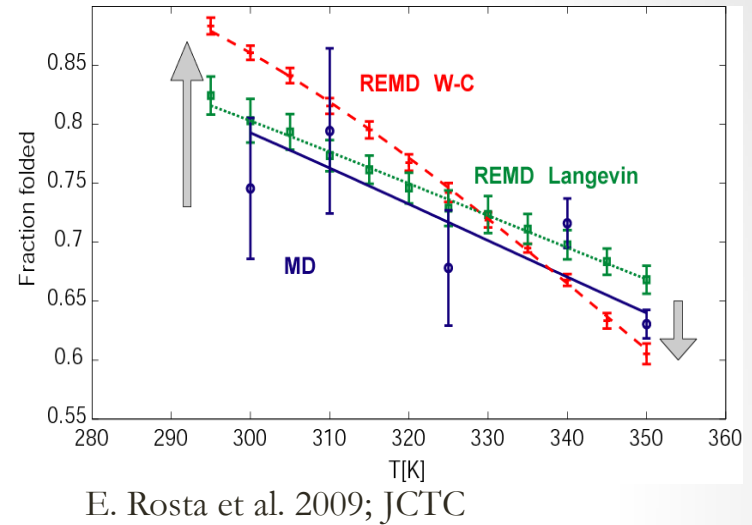
$$\eta = \frac{\sigma_{MD}^2(Nt_{sim})}{\sigma_{REMD}^2(t_{sim})} = \frac{\sigma_{MD}^2(t_{sim})}{N\sigma_{REMD}^2(t_{sim})}$$

- Estimate of the error of a general property Y :

$$Y(t) \cong (\langle Y \rangle_F - \langle Y \rangle_U)s(t) + \langle Y \rangle_U \Rightarrow \text{var}(\bar{Y}) \cong (\langle Y \rangle_F - \langle Y \rangle_U)^2 c_s(t)$$

- Error in estimating the folding probability, \bar{s} :

$$\sigma^2(t_{sim}) = \text{var}(\bar{s}) = \frac{2}{t_{sim}^2} \int_0^{t_{sim}} (t_{sim} - t) c_s(t) dt$$



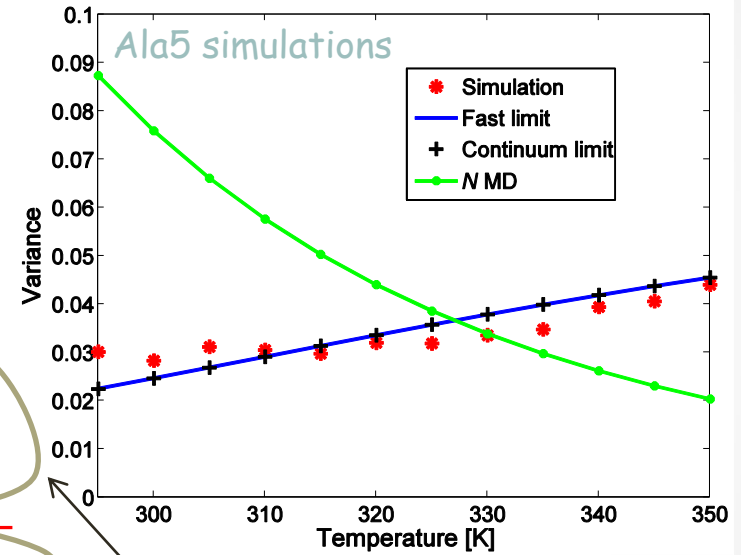
Efficiency of Replica Exchange

$$\eta = \frac{\sigma_{MD}^2(Nt_{sim})}{\sigma_{REMD}^2(t_{sim})} = \frac{\sigma_{MD}^2(t_{sim})}{N\sigma_{REMD}^2(t_{sim})}$$

$$\left. \begin{aligned} \sigma_{MD}^2(t_{sim}) &= \frac{2}{t_{sim}} \frac{p_{F_1} p_{U_1}}{\lambda_1} \\ \sigma_{REMD}^2(t_{sim}) &= \frac{2}{t_{sim}} \frac{p_{F_1}^2 p_{U_1}^2}{\sum_{i=1}^N p_{F_i} k_{U_i}} \end{aligned} \right\}$$

$$\eta_1 = \frac{\sum_{i=1}^N p_{F_i} k_{U_i}}{N p_{F_1} k_{U_1}}$$

Number of transitions at target temperature (T_1)



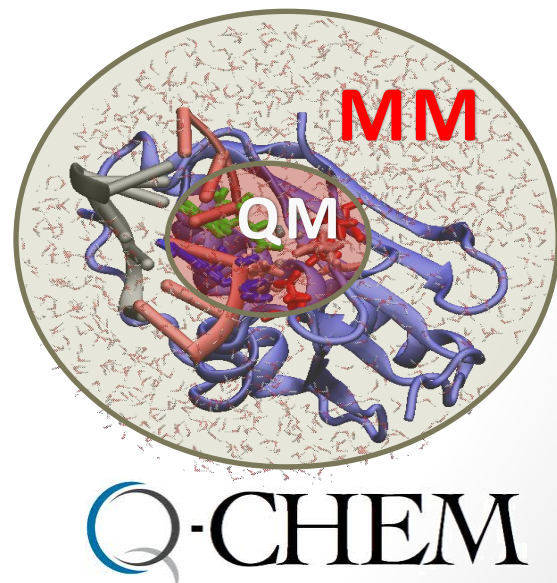
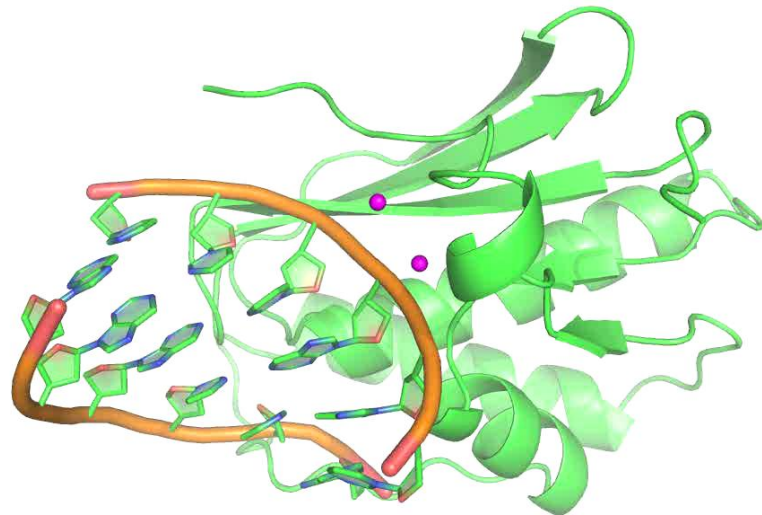
Average number of transitions over all temperatures

Results I: Kinetic Modeling

- Analytical efficiency expression is derived for *replica exchange & simulated tempering* simulations in the limit of fast exchange.
- Efficiency for slow exchange is obtained by numerical solution of the full kinetic rate matrix problem.
- Replica exchange & simulated tempering simulations have identical efficiencies in the limit of fast exchange.
- Model provides guidance for optimal simulation protocol to minimize the statistical error (e.g., T-spacing, exchange frequency, etc.).

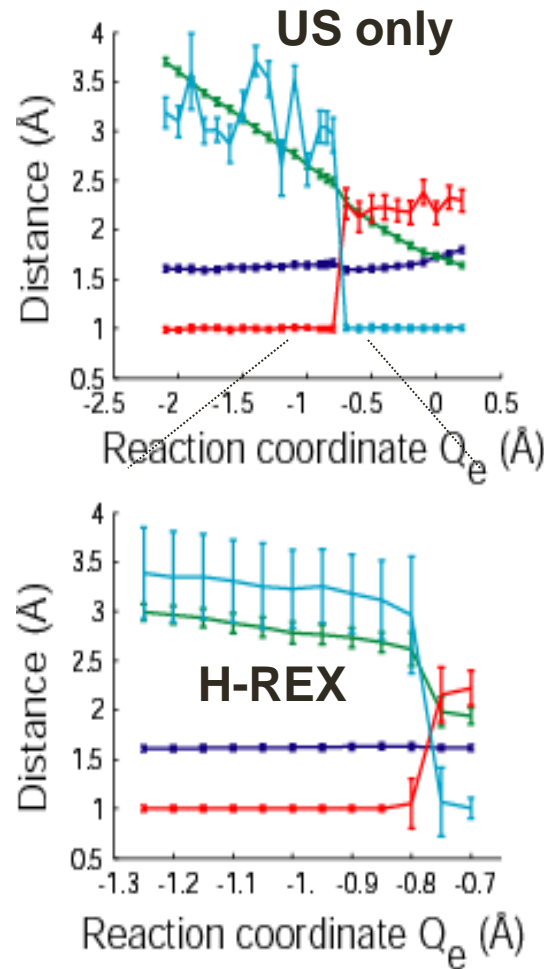
Computational Methods

- NEW QM/MM implementation with **Q-Chem** +CHARMM using full electrostatic embedding
Woodcock et al., J. Comp. Chem., 2007
- Phosphate-diester hydrolysis by attacking water
- DFT B3LYP method
- **Free energy** calculations using Umbrella Sampling
- COUPLED WITH HAMILTONIAN REPLICA EXCHANGE

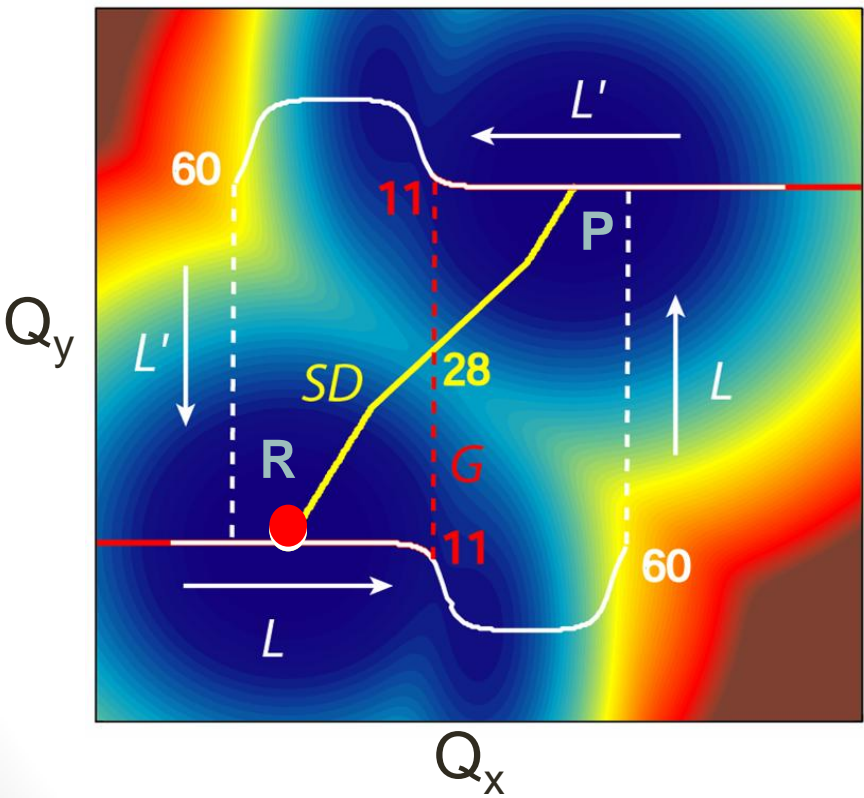


Hamiltonian replica exchange

- Smoother curves – better sampling
- Does not add extra cost to the simulations
- Discontinuity problem is not solved – could not help overcome proton transfer barrier



Hysteresis in low dimensional reaction coordinates

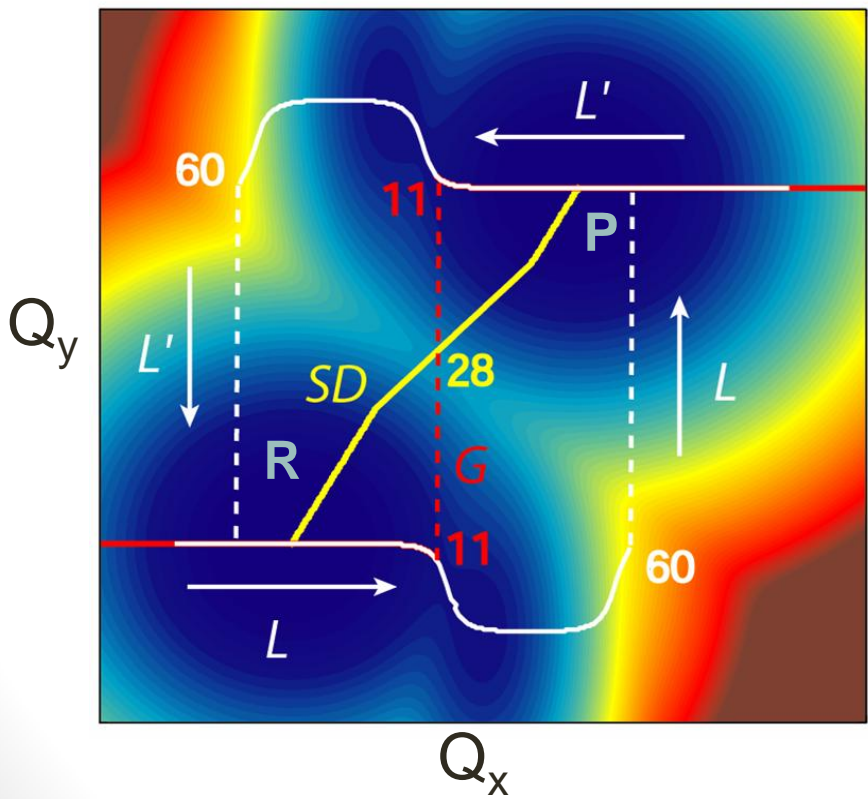


Energy minimizations along Q_x :

(Fix value along Q_x , minimize along all other coordinates.)

- **Steepest Descent (SD):**
 - Passes through transition state
 - Computationally not feasible
- **Local search (L):**
 - Overestimates barrier
 - Shows hysteresis
- **Global search (G):**
 - Underestimates barrier
 - Characterized by discontinuity

Hysteresis in low dimensional reaction coordinates



Free energy calculations:

Perfect sampling
+ wrong reaction coordinate
= underestimate the barrier of
the 1D (PMF) free energy
profile -- **Characterized by
discontinuity**

$$e^{-G(Q_x)/k_B T} =$$

$$\int dQ_y e^{-G(Q_x, Q_y)/k_B T}$$

Hamiltonian replica exchange

- Smoother curves – better sampling
- Does not add extra cost to the simulations
- Discontinuity problem is not solved – could not help overcome proton transfer barrier

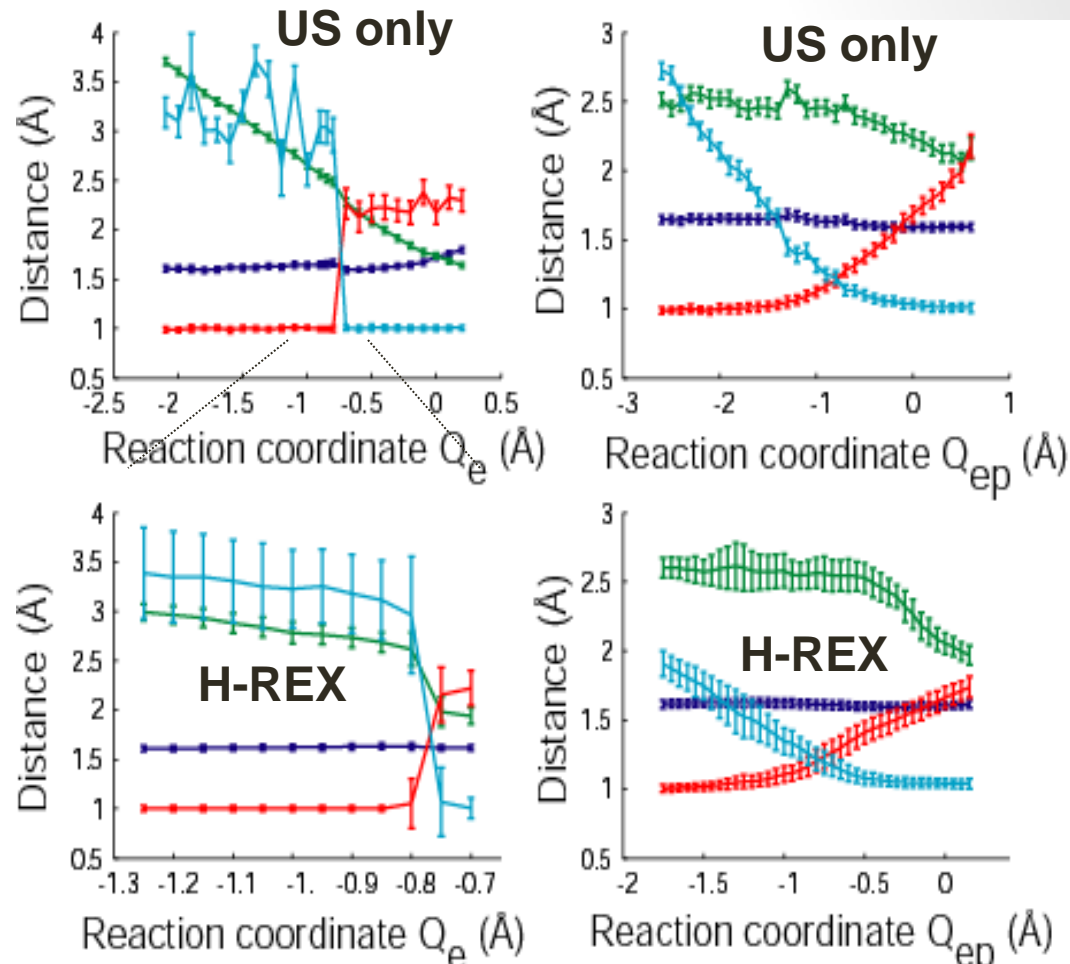
Electron transfer:

$$Q_e = r_1 - r_2$$

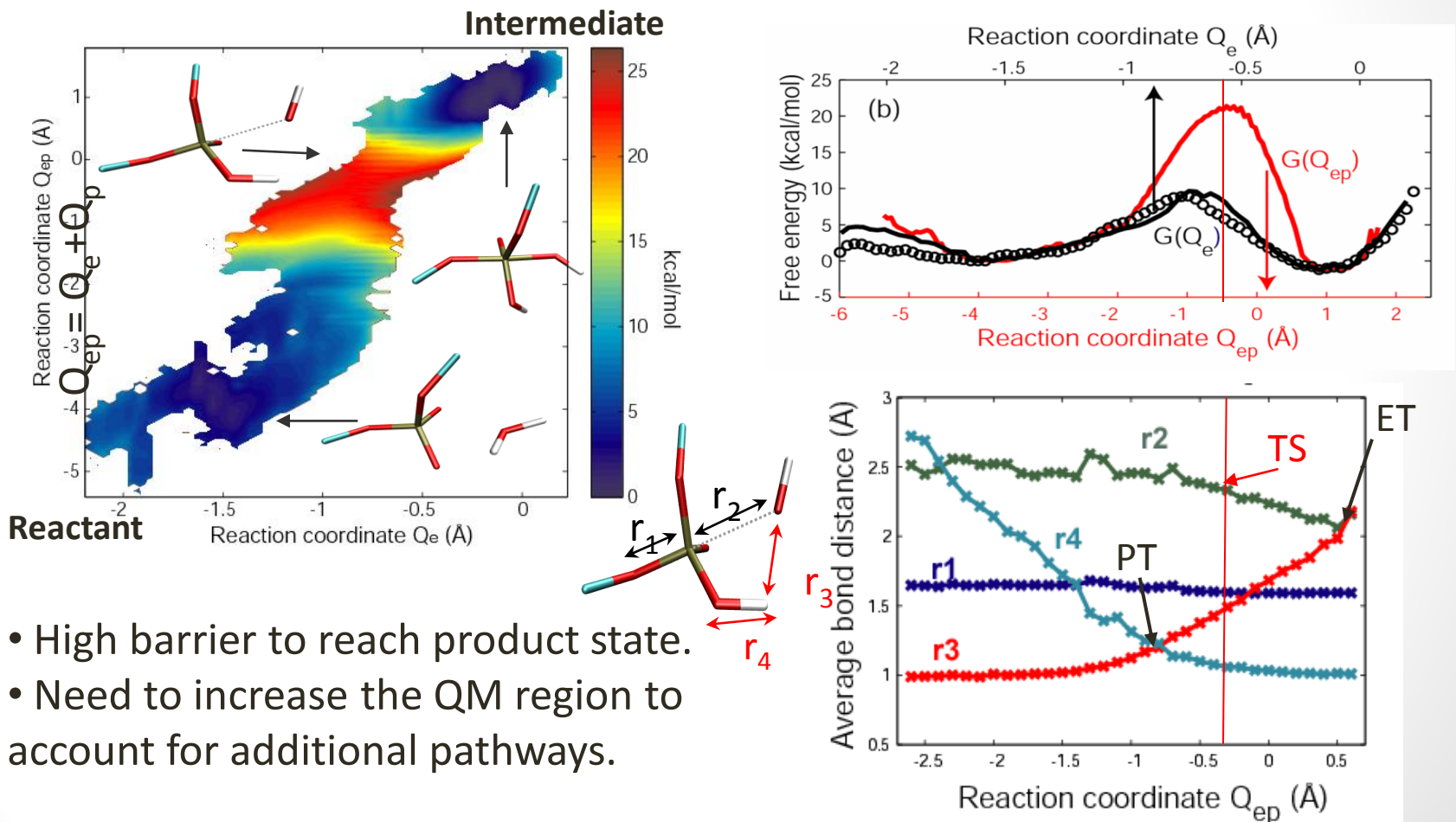
Proton transfer:

$$Q_p = r_3 - r_4$$

New coordinate for additional 1D umbrella sampling: $Q_{ep} = Q_e + Q_p$



2D-WHAM with proton transfer + electron transfer coordinate, Q_{ep}

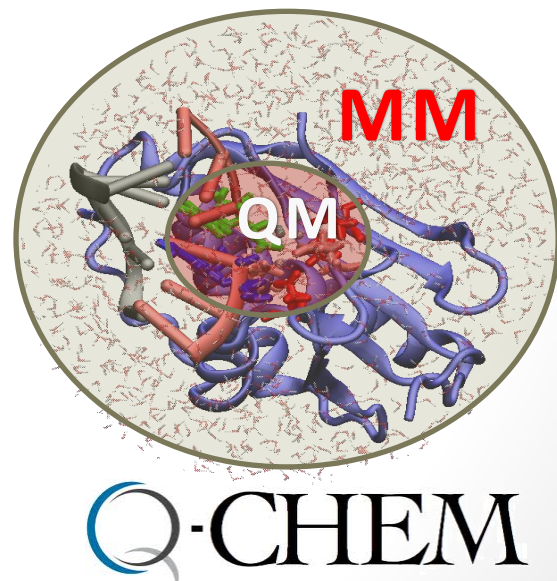
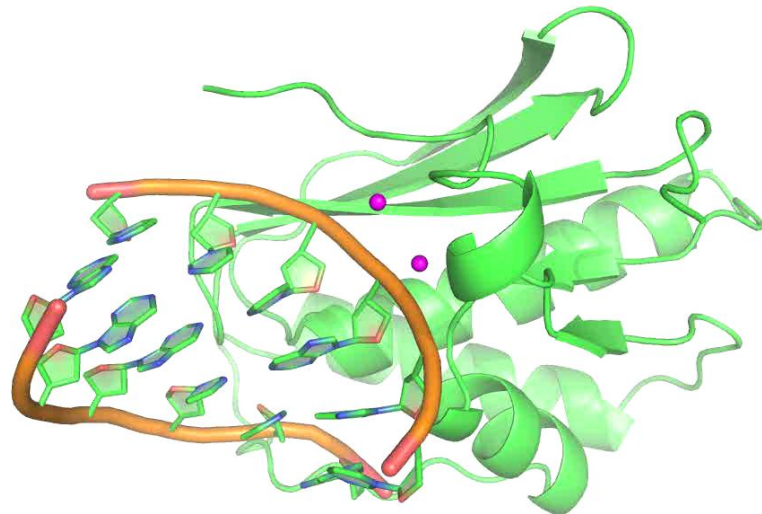


- High barrier to reach product state.
- Need to increase the QM region to account for additional pathways.

First proton transfer, then ET (bond breaking/forming at P)

Computational Methods

- NEW QM/MM implementation with **Q-Chem** +CHARMM using full electrostatic embedding
Woodcock et al., J. Comp. Chem., 2007
- Phosphate-diester hydrolysis by attacking water: QM region with 91 atoms
- DFT B3LYP method (6-31+G* basis)
- **Free energy** calculations of the reaction with enhanced sampling methods: Hamiltonian replica exchange coupled with **finite temperature string** method

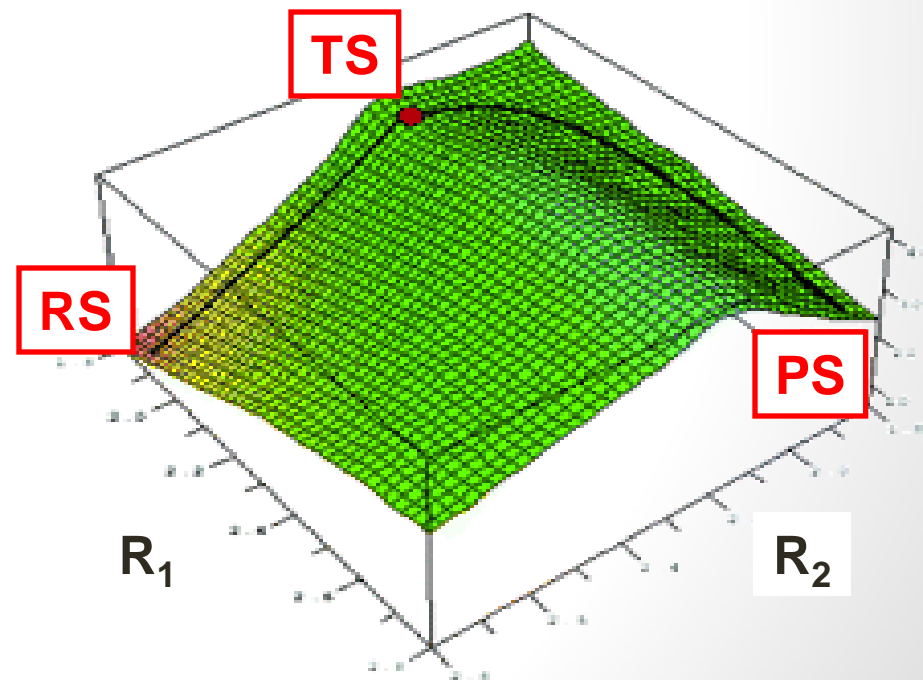


Free Energy Simulations Using the String Method

- Optimized a **1D string** in the **multidimensional space of the internal reaction coordinates** to obtain minimum free energy path

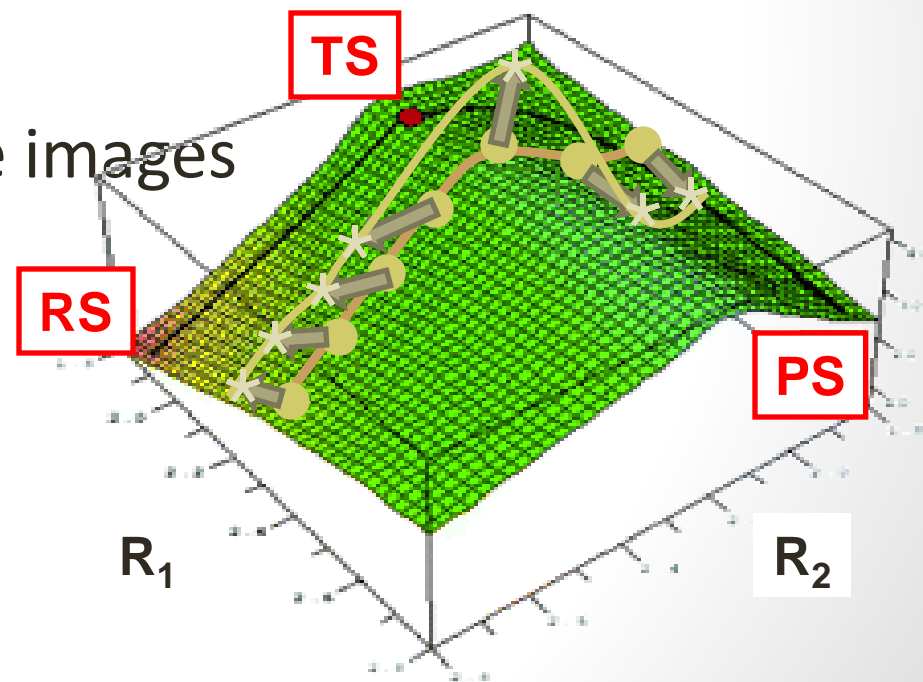
E, Ren, Vanden-Eijnden, *Phys. Rev. B*, 2002

- Hamiltonian replica exchange between string images



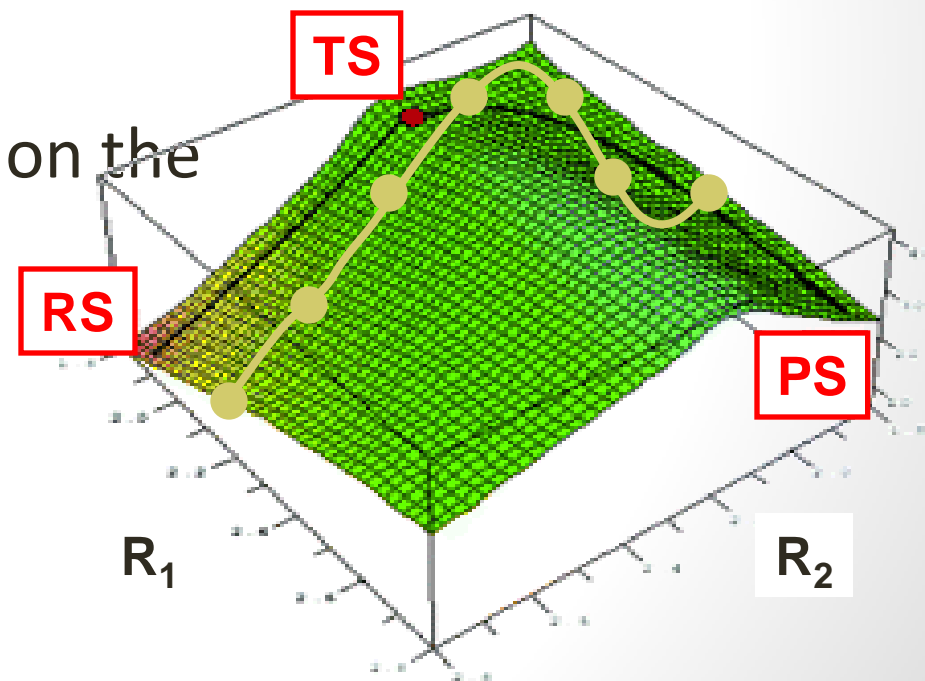
Free Energy Simulations Using the String Method

- Start with a guess for the string
- Run Umbrella Sampling simulations
- Determine forces for the images along the string
- Fit new string



Free Energy Simulations Using the String Method

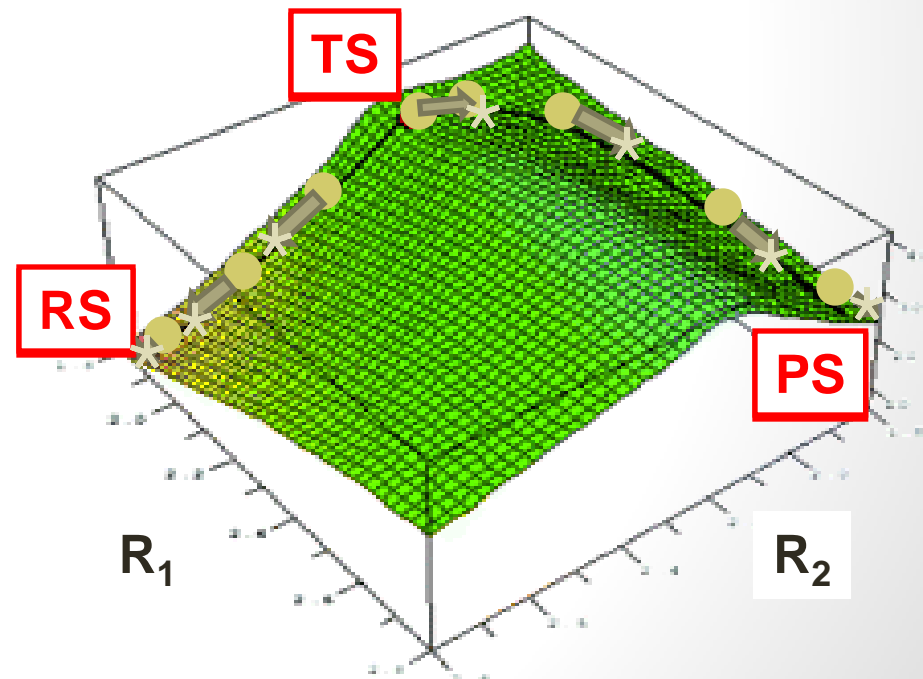
- Start with a guess for the string
- • Run Umbrella Sampling simulations
- Determine forces acting on the images along the string
- Fit new string
- Redistribute images
- Run next iteration



Free Energy Simulations Using the String Method

- Converged string:
 - Forces are parallel to string
- We use **all data** from all string simulations with **Histogram Free** implementation of **WHAM** (**MBAR**): works with **very high dimensionality**

$$f_m^{-1} = \sum_{k=1}^{NSim} \sum_{A \in NSim} \frac{c^m(\xi_A^k)}{\sum_{l=1}^{NSim} N_l f_l c^l(\xi_A^k)}$$



Proton Transfer Pathways

- **Step I. Deprotonation of water**

- a. via downstream phosphate group
- b. via Glu188
- c. via cleaved phosphate

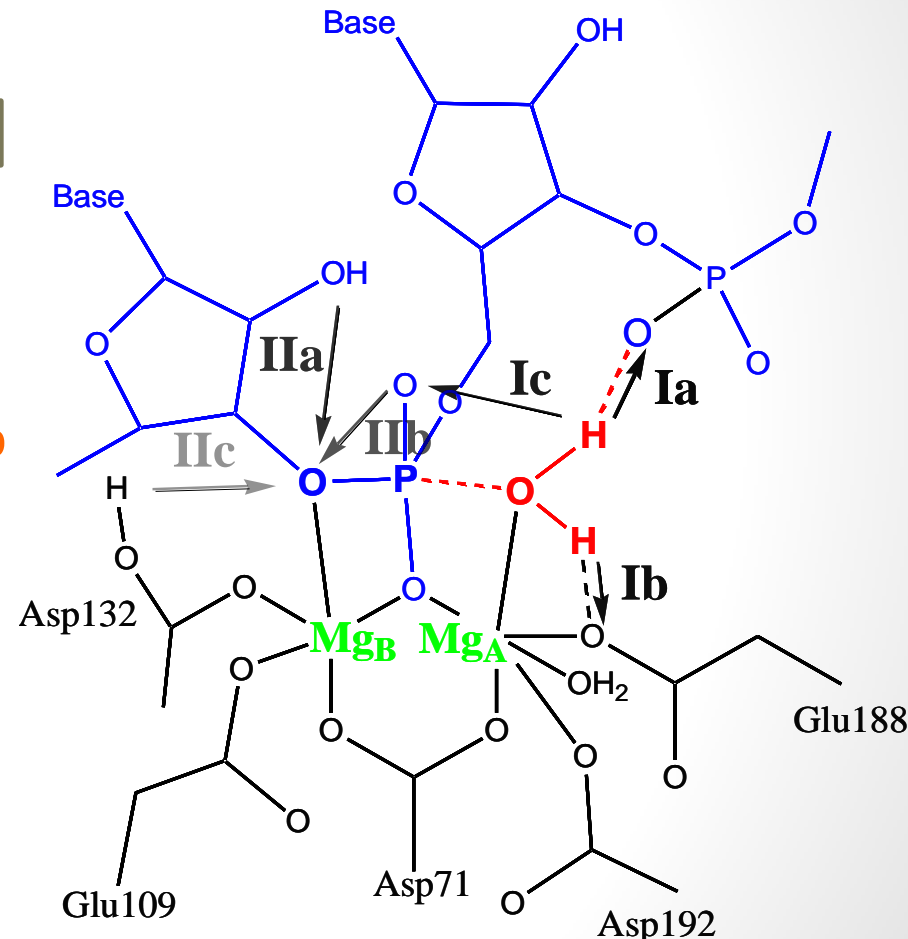
De Vivo et al. JACS, 2008

- **Step II. Protonation of leaving group**

- a. via 2'OH of sugar
- b. via cleaved phosphate
- c. via conserved Asp132

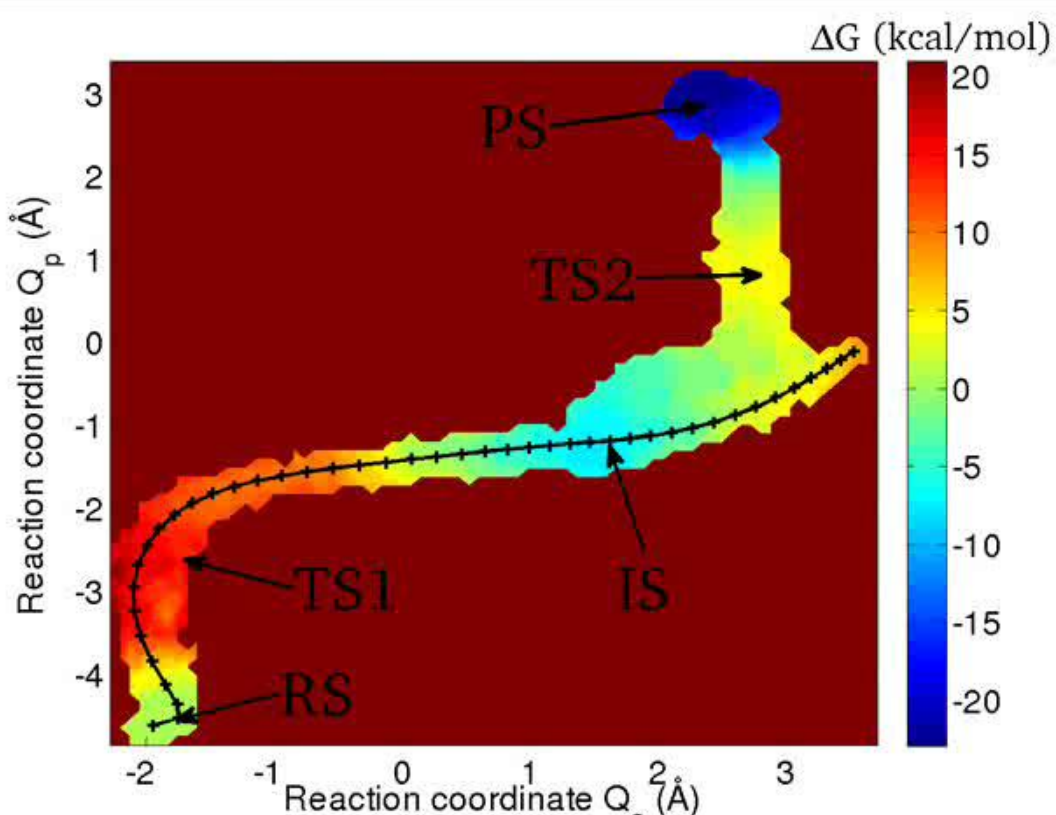
Thiol substitution experiments on the accepting **O** atom show a nearly **10-fold reduction** in reaction rate.

Haruki et. al., *Biochemistry*, 2000



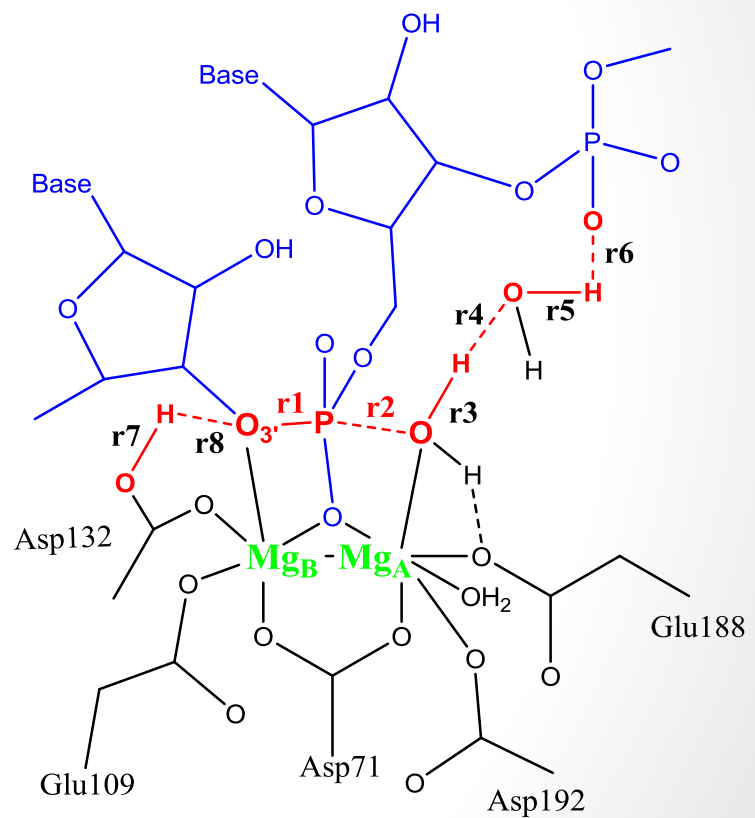
Rosta, Nowotny, Yang, Hummer,
J. Am. Chem. Soc., 2011

RNase H: Free Energy Surface

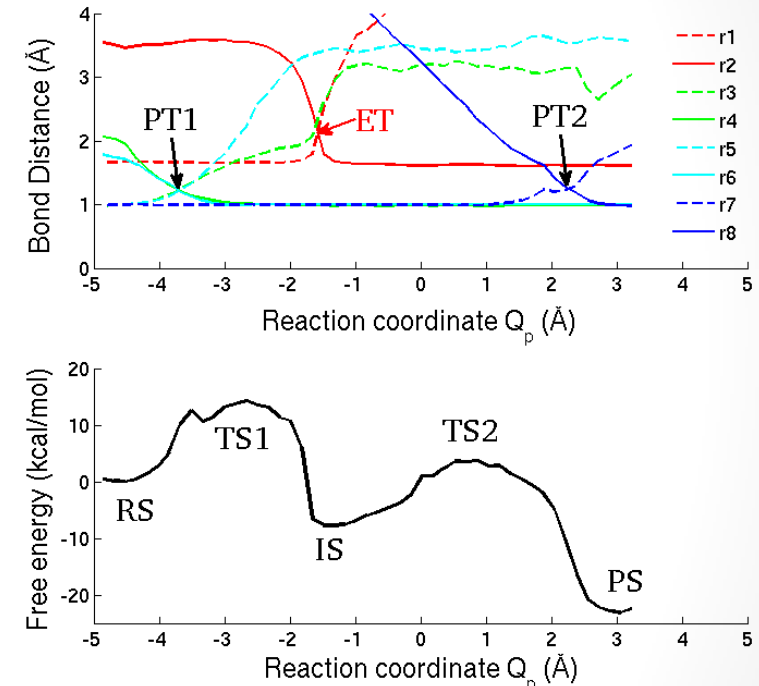
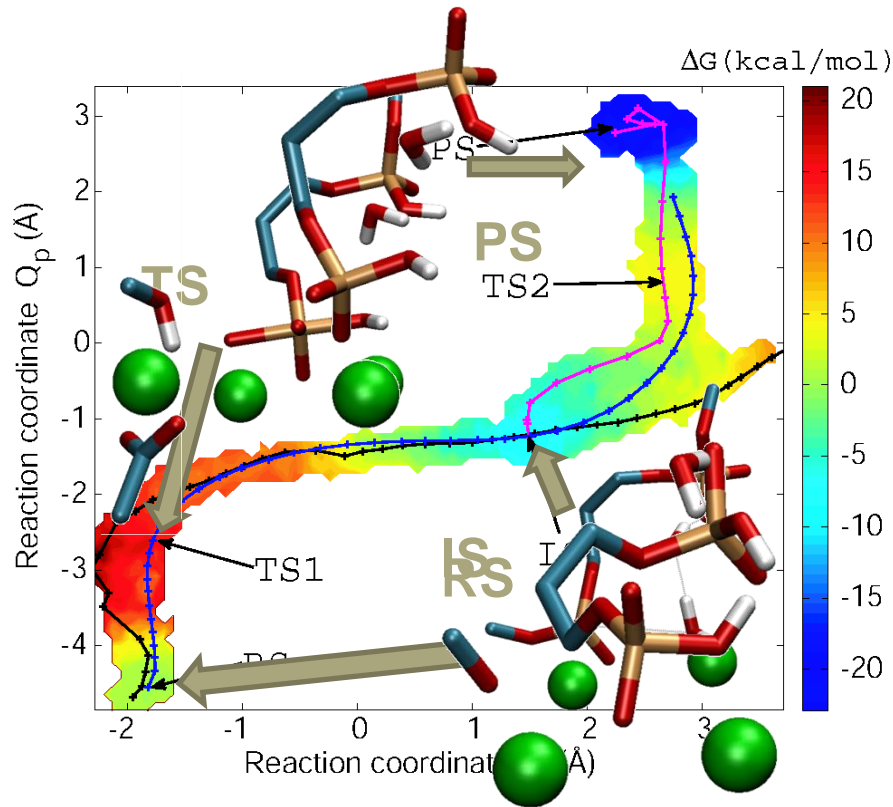


$$Q_e = r_1 - r_2$$

$$Q_p = r_3 - r_4 + r_5 - r_6 + r_7 - r_8$$



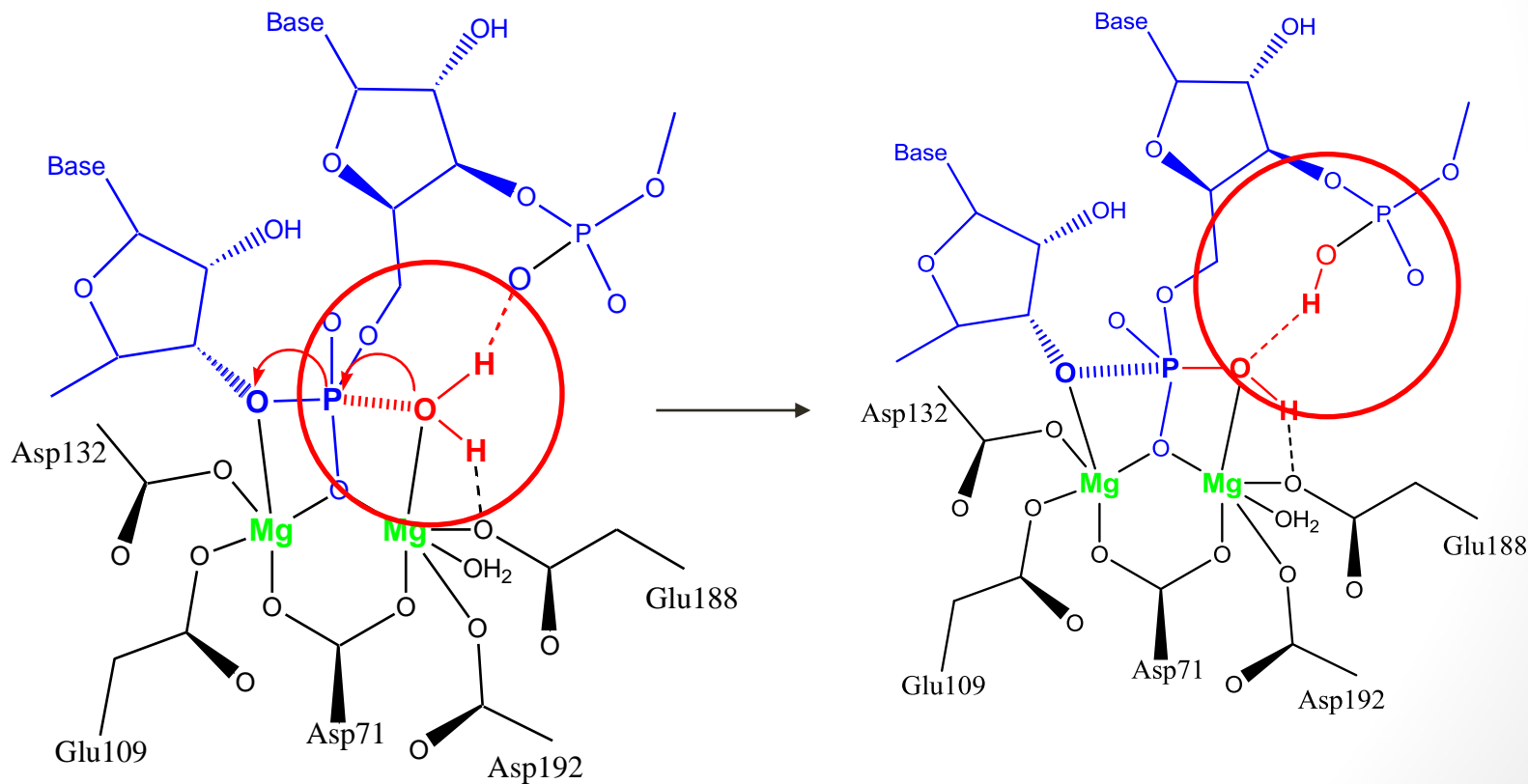
Free Energy Surface



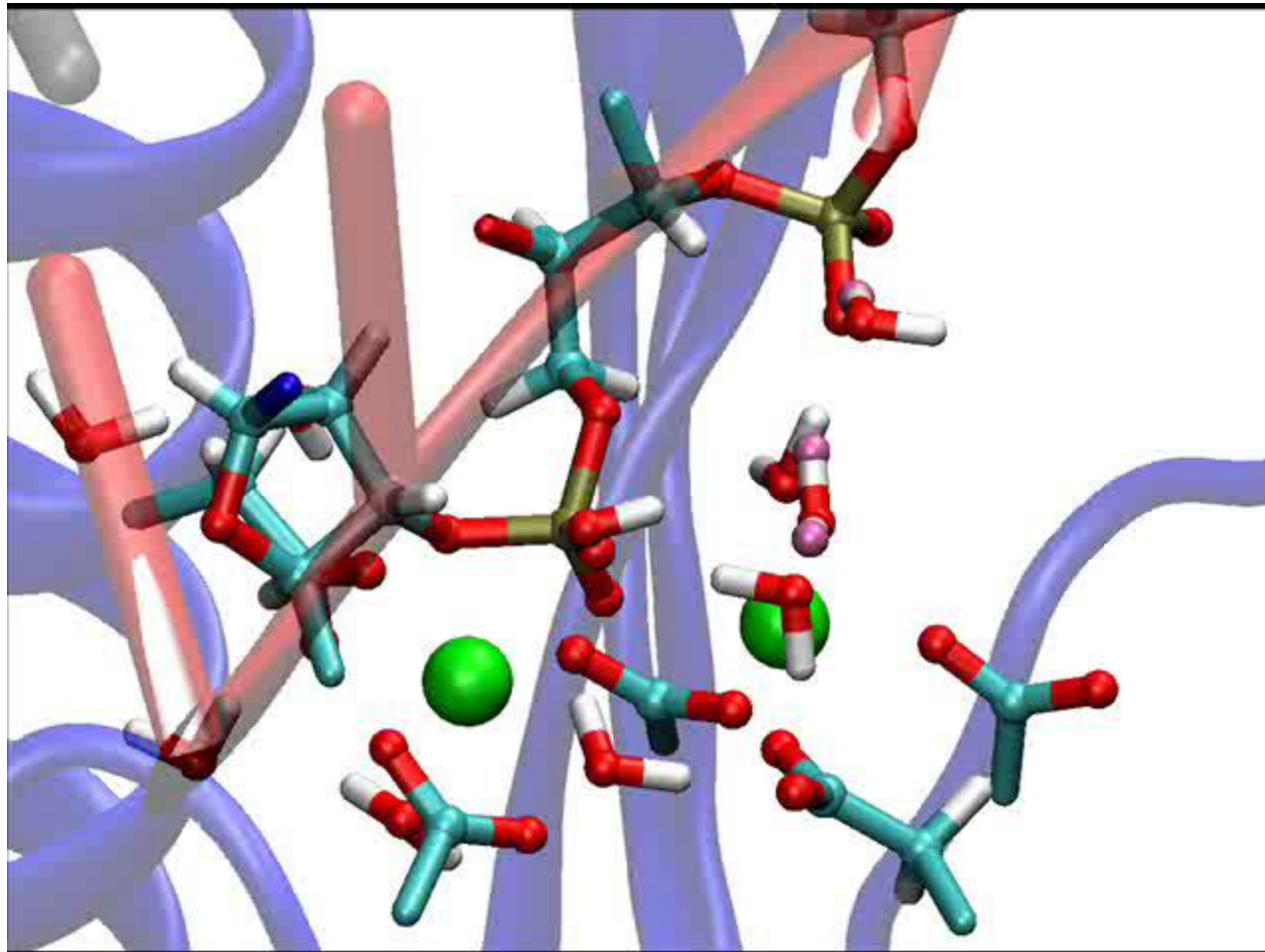
It has been thought that proton transfer is generally facile, however, we find that

barriers are dominated by proton transfer!

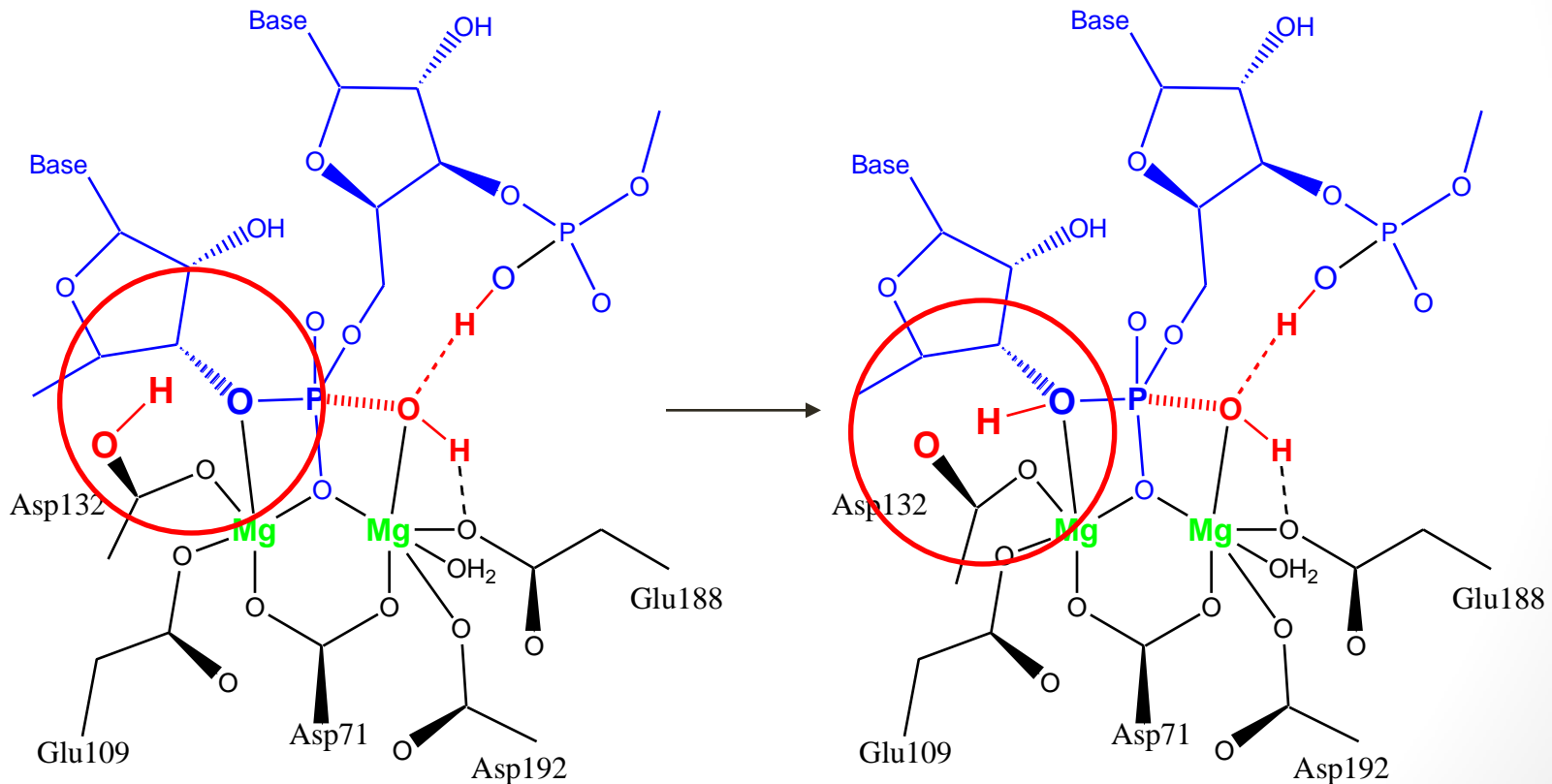
RNase H: Mechanism for Deprotonation (Step 1)



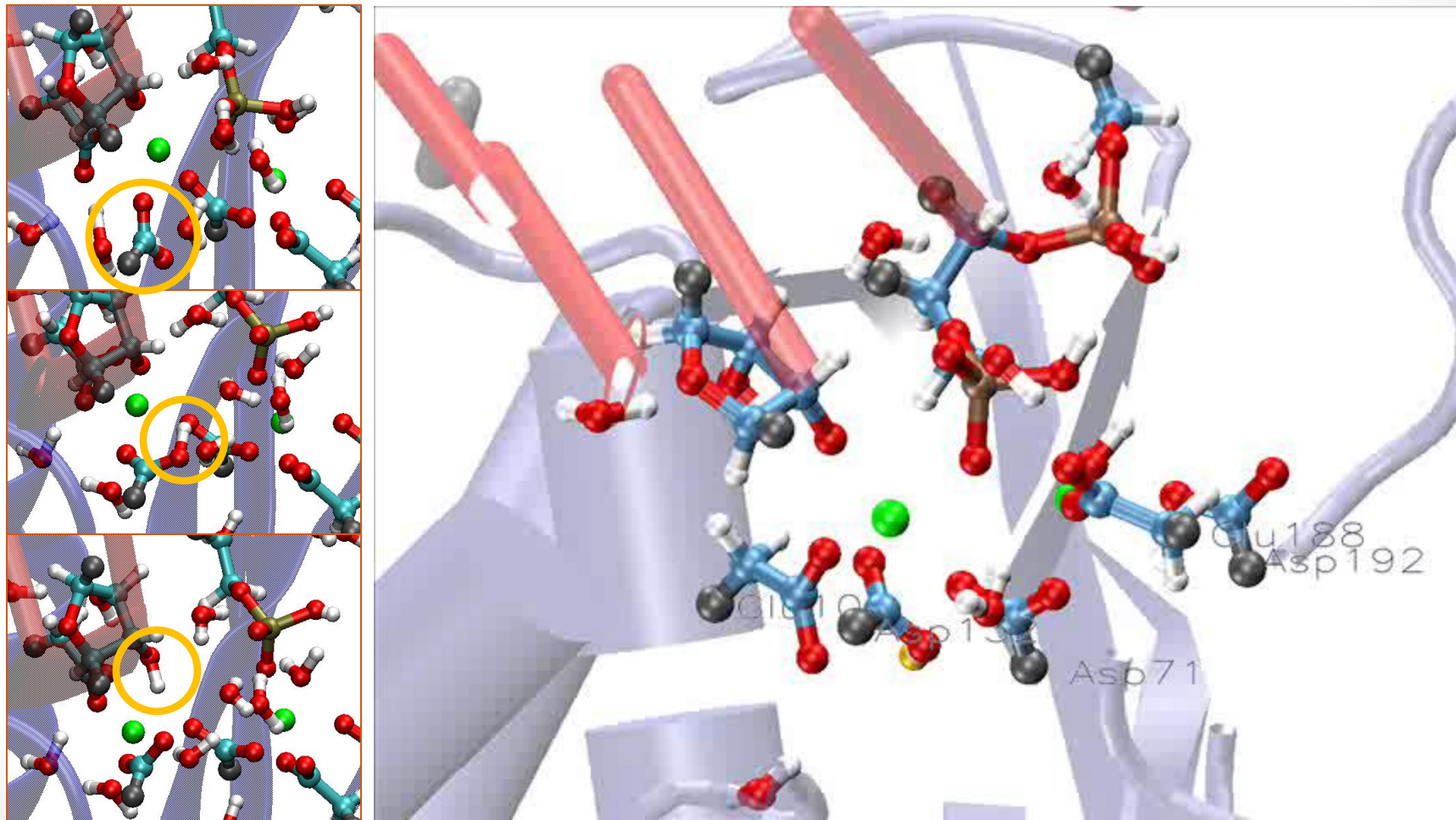
RNase H: Deprotonation via Downstream Phosphate



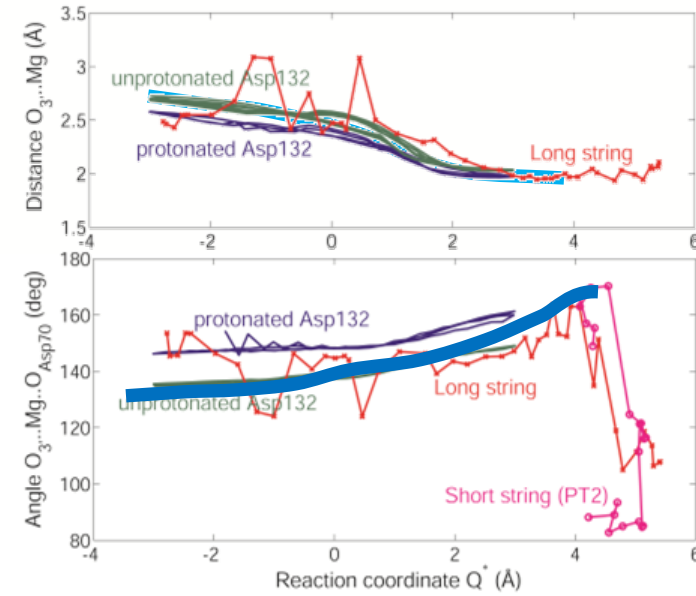
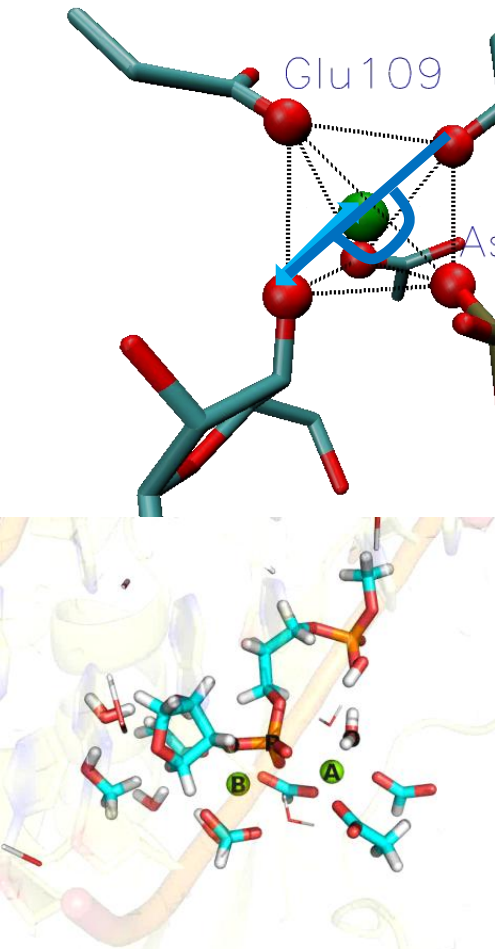
RNase H: Mechanism for Protonation (Step 2)



Product Formation *via* Asp132

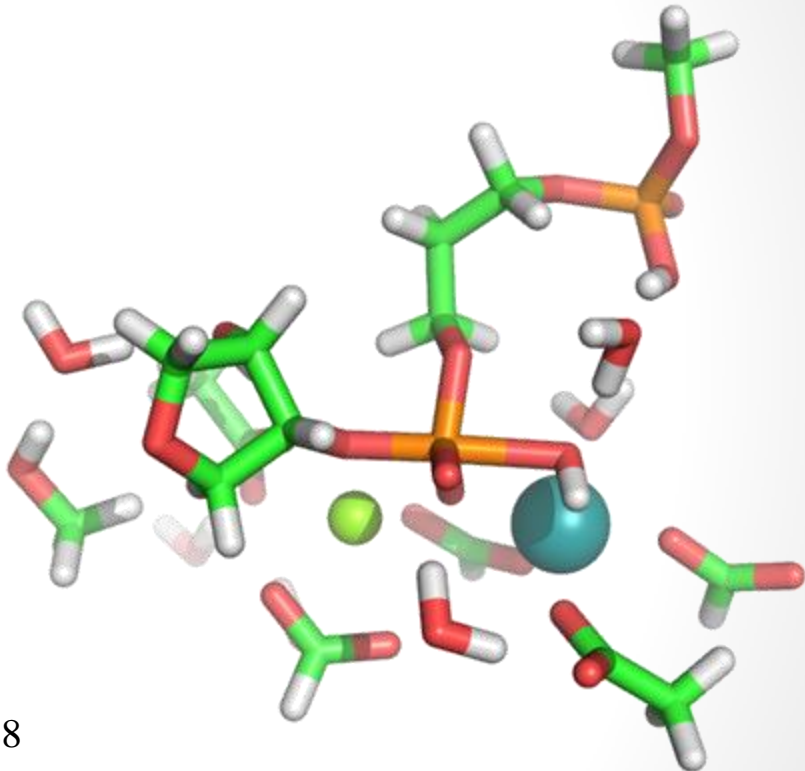
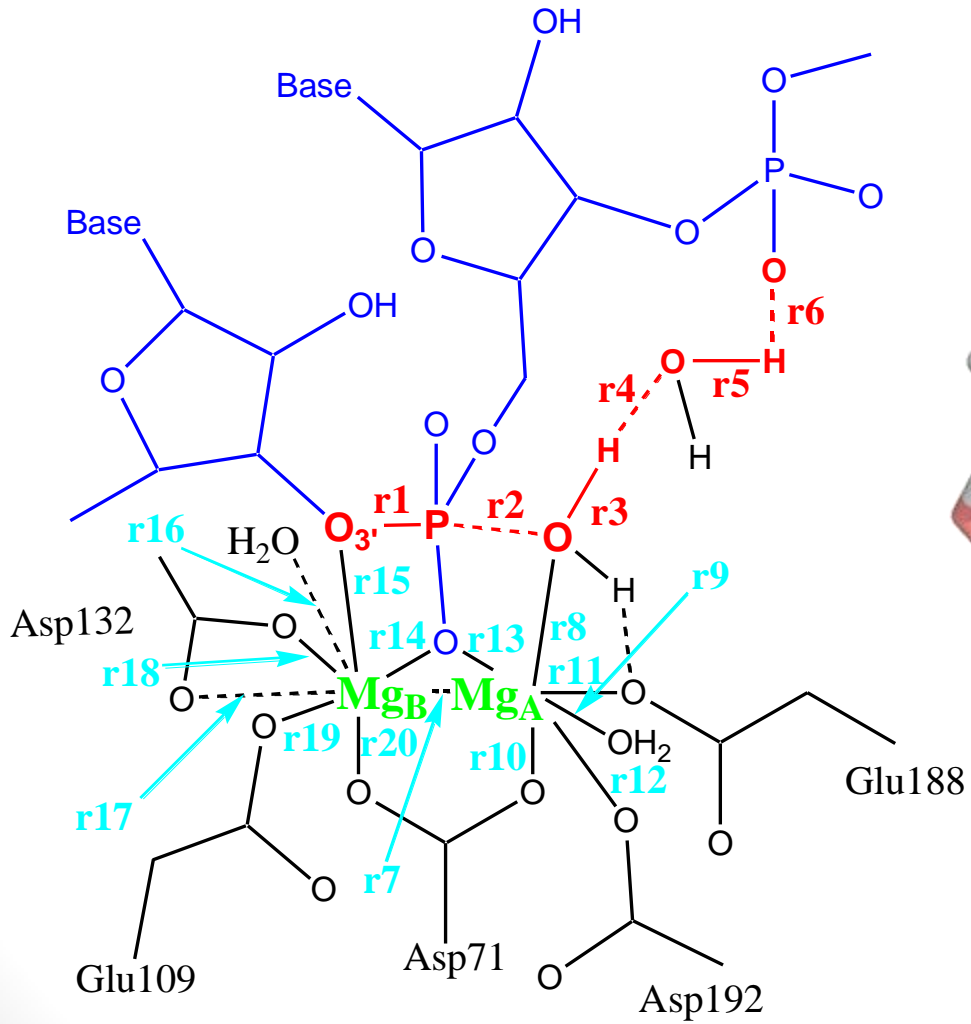


Pentacoordinated Mg^{2+} -ion B becomes more symmetrical @ TS



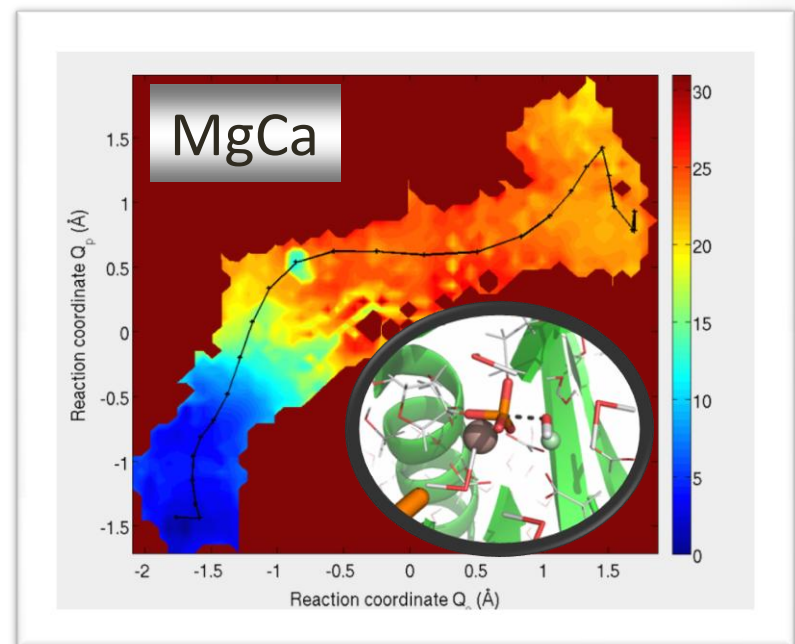
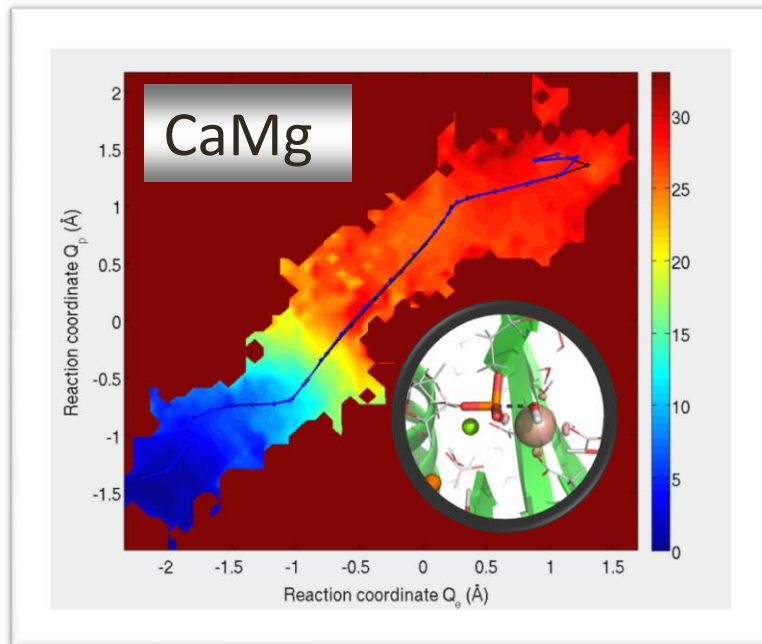
- More symmetric coordination of Mg^{2+} -ion B lowers the TS energy
- Shorter distance of Mg^{2+} -ion B to the leaving group stabilizes the negative charge by lowering the pK_a of the leaving group

Single Metal-Ion Substitutions: QM Region and Reaction Coordinates

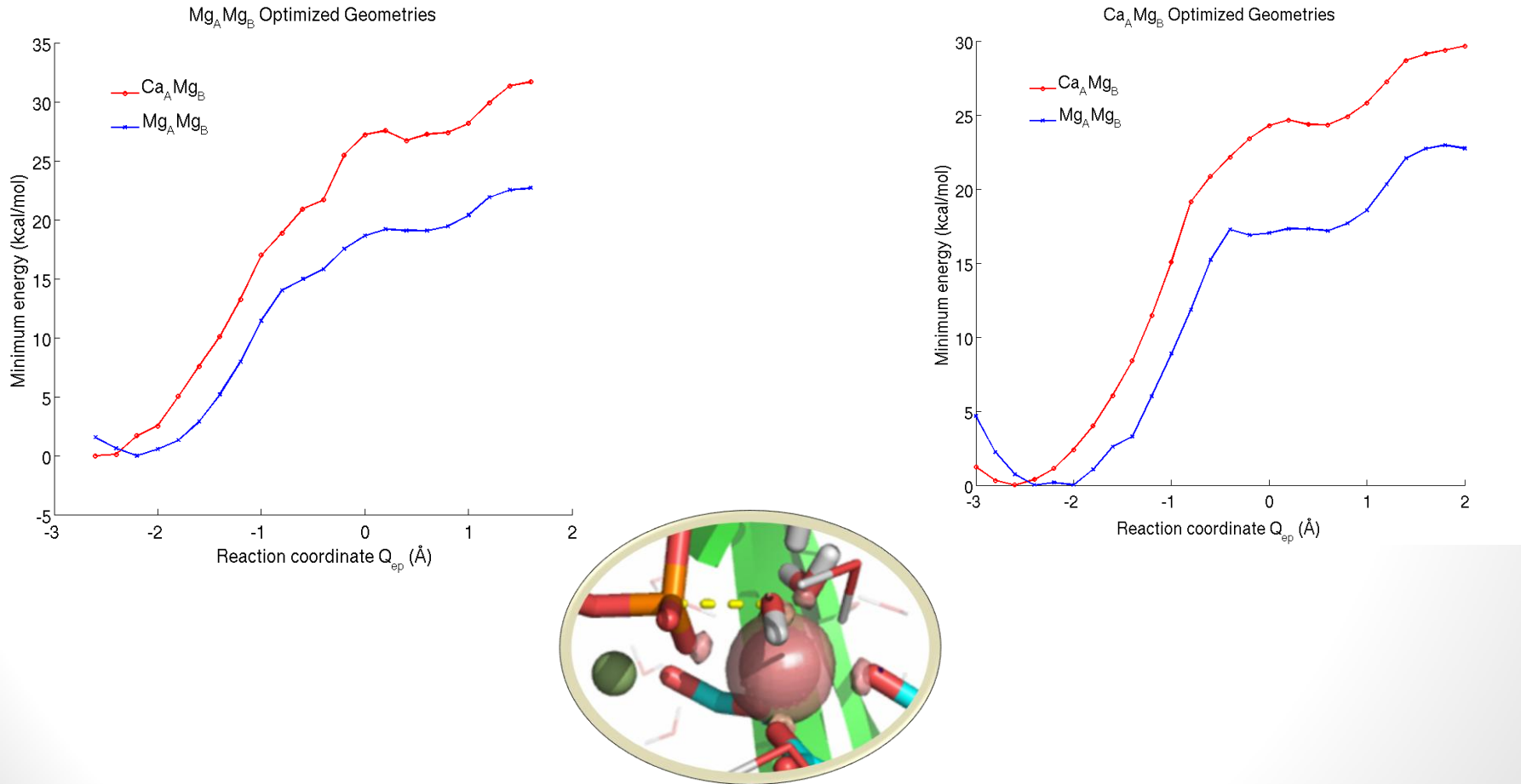


Substitutions at single metal ion sites: Mg^{2+} vs. Ca^{2+}

Replacing either Mg^{2+} metal ions by Ca^{2+} abolishes catalysis.

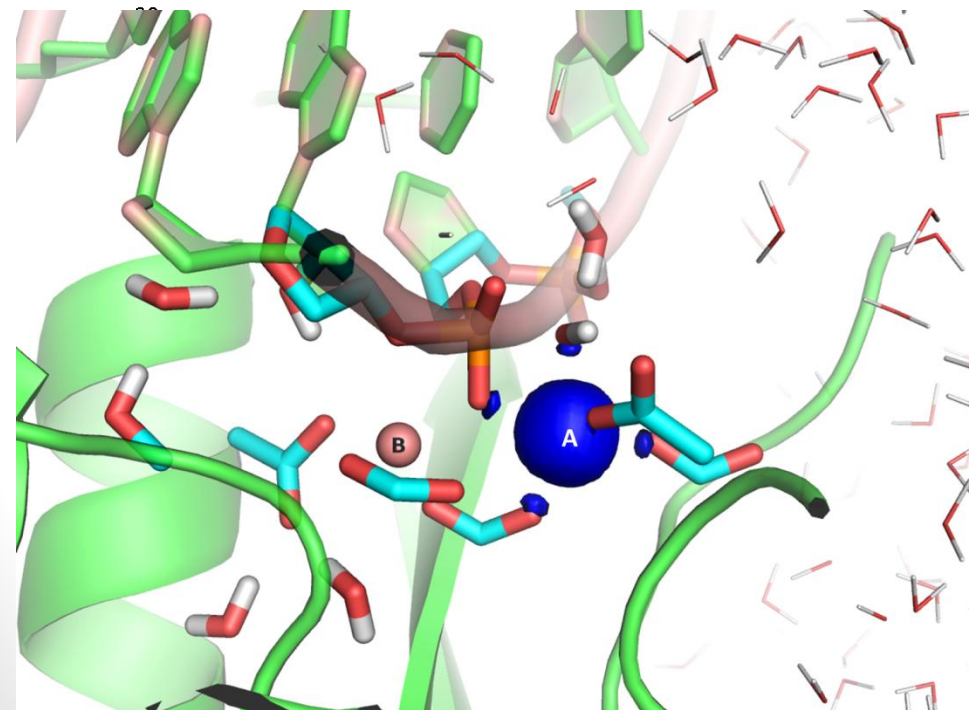
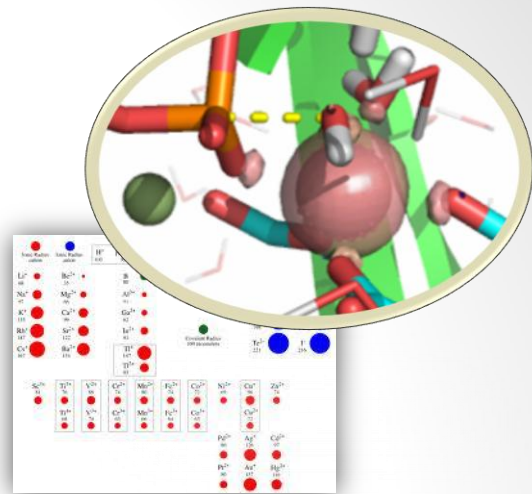


Metal Ion A Site: Geometric effects do not play a major role



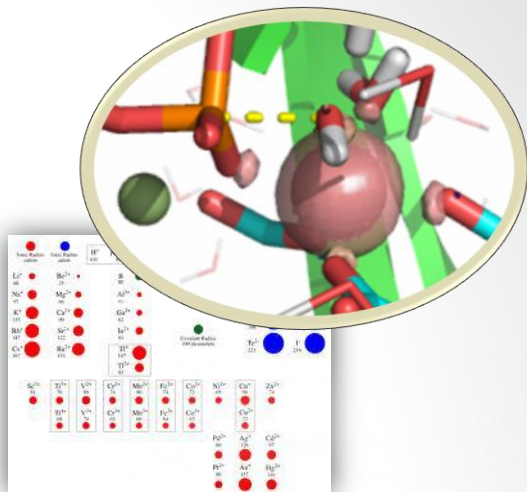
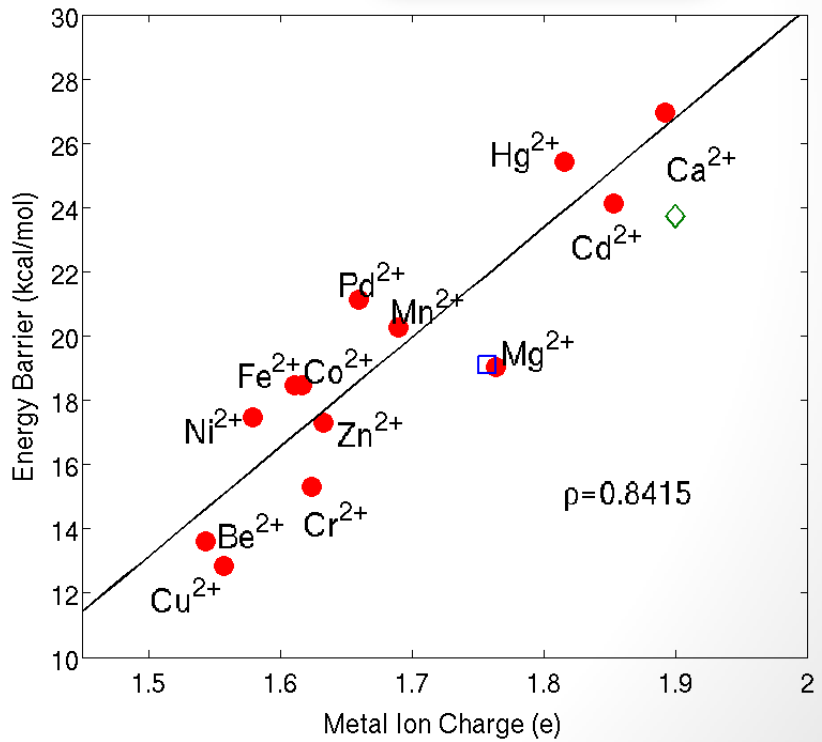
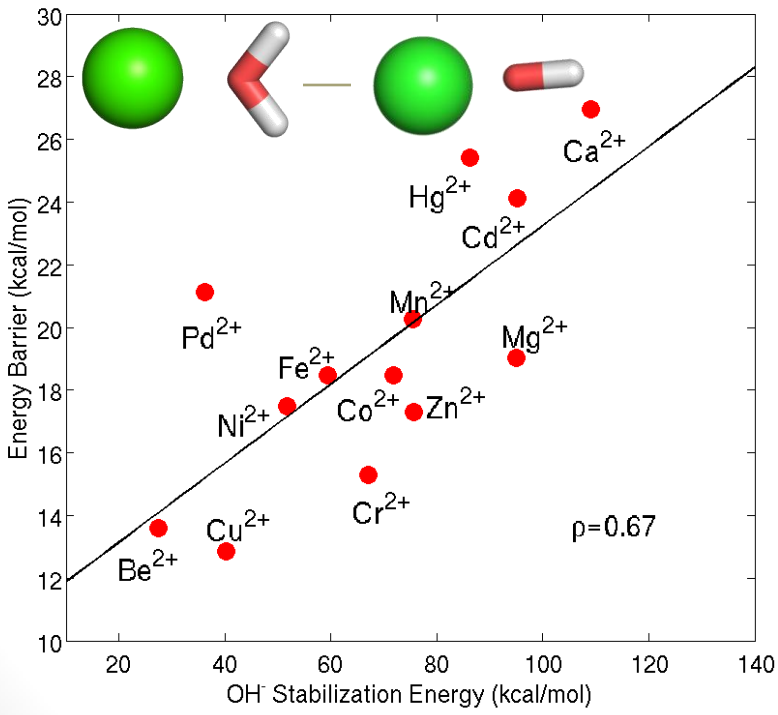
Role of partial charge transfer to metal ion A

Substitutions at metal ion A site with a series of divalent metal ions using Mg-optimized reaction pathway. (aug-cc-pVTZ(PP) basis set)

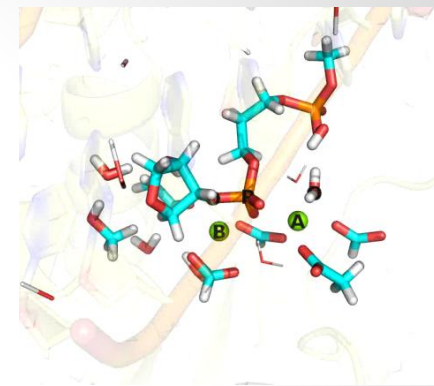


Role of metal ion A

Substitutions at metal ion A site with a series of divalent metal ions using Mg-optimized reaction pathway.



Summary



- A multidimensional finite temperature string reaction coordinate method is developed for QM/MM free energy calculations with application to RNase H.
- Hamiltonian Replica Exchange is extended to enhance sampling with *String Free Energy* simulations.
- Several PT mechanistic pathways are identified in RNase H catalytic reaction. The reaction barrier (rate) agrees well with experiment for the most probable path.
- PT dominates the reaction barrier suggesting that enzymes use metal ions to help lower the pK_a of attacking and leaving groups.
- High resolution TS structures can be used in further simulations for predicting changes in catalysis upon perturbations such as *binding of drug molecules*

Acknowledgements

Gerhard Hummer

(**Laboratory Of Chemical Physics, NIDDK, NIH**)

X-Ray crystallography:

Wei Yang (LMB, NIDDK, NIH)

Marcin Nowotny (IIMCB, Warsaw)

Kinetic theory:

Attila Szabo (LCP, NIDDK, NIH)

CHARMM + Q-Chem:

Bernard Brooks (NHLBI, NIH)

Lee Woodcock (USF, Tampa)

Yihan Shao (Q-Chem)

